


25X1A



25X1A


#6

REPORT 974-012-2

Final Report on the Design Study
of a Self-Powered Air Bearing.

October 1965

25X1A



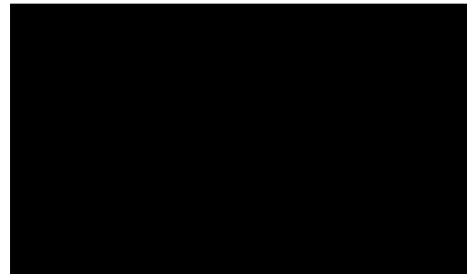
FOREWORD

25X1A

[REDACTED] submits this report in compliance with Part II of the
Contract Brief of Contract No. [REDACTED]

25X1A

25X1A



Approved

ABSTRACT

The purpose of this assignment was to study the feasibility of an air bearing in which the power source would be incorporated as an essential part of the design. A test bed was built in the first phase of the program under Contract No. 974, as described in Report No. 974-012-1. In this report a summary of earlier investigations is given for convenience.

Due to the allocation of priorities to other assignments, many possible configurations were not evaluated, but sufficient testing was completed to permit some conclusions and recommendations to be made.

CONTENTS

SECTION	PAGE
1. INTRODUCTION	1-1
2. SUMMARY OF PRECEDING PROGRAM	2-1
2.1 Self-Powered Air Bearing	2-1
3. CONTINUATION OF STUDY PROGRAM	3-1
3.1 Technical Discussion	3-1
3.1.2 Air Bearing Test Bed	3-1
3.1.3 Power Generators	3-2
3.1.4 Performance Data	3-4
3.1.5 System Characteristics	3-4
3.1.6 Principal System Elements	3-11
3.1.6.1 Bearing Cage	3-11
4. TEST PROGRAM	4-1
4.1 Test #1. Quadruple Fan Installation	4-1
4.1.1 Efficiency of Configuration	4-8
4.2 Blower Wheel Installations	4-9
4.2.1 Test #2. Twin 3.81-Inch Diameter Blower Wheels	4-9
4.2.2 Efficiency of Configuration	4-10
4.3 Test #3. Twin 3.81-Inch Diameter Blower Wheels	4-13
4.3.1 Efficiency of Configuration	4-15
4.4 Test #4. Twin 3.81-Inch Diameter Blower Wheels - Position 1 With Intake Restrictors	4-21

CONTENTS (cont'd)

SECTION	PAGE
4.4.1 Efficiency of Configuration	4-21
4.5 Test #5. Twin 3.81-Inch Diameter Blower Wheels With Intake Fairings	4-23
4.6 Test #6. Twin 3.81-Inch Diameter Blower Wheels With Intake Restrictors and Two 2.50-Inch Diameter Blower Wheels in Center of Bearing	4-25
4.7 Test #7. Pressure and Flow Tests	4-29
5. SUMMARY AND CONCLUSIONS	5-1
5.1 Summary	5-1
5.2 Conclusions	5-4

ILLUSTRATIONS

FIGURE		PAGE
2-1	Air Bearing Using Transverse Flow Fan	2-2
2-2	Scheme of Air Bearing with Transverse-Flow Fan	2-4
2-3	Layout of Air Bearing Test Bed	2-5
2-4	Air Bearing Test Bed Showing Fan Installed and Wheel	2-6
2-5	Perforated Cage	2-7
2-6	Air Bearing Test Bed Showing Fan Installation	2-8
3-1	Bearing on Test Tank	3-3
25X1A 3-2	Performance Curves of [REDACTED] Four-Bladed, 4-Inch Diameter Fans	3-5
25X1A 3-3	Performance Curves of [REDACTED] Forward-curved, 3.81-Inch Diameter Blower Wheels	3-6
25X1A 3-4	Performance Curves of [REDACTED] Forward-Curved, 2.50-Inch Diameter Blower Wheels	3-7
3-5	Graph for Determining Type of Fan for a Specific Application	3-9
4-1	Test Bed Impeller Configurations	4-2
4-1 (cont'd)	Test Bed Impeller Configurations	4-3
4-2	Bearing Support Characteristics	4-5
4-3	Effect of Wheel Location on Pressure Profile of Cushion	4-16
4-4	Supported Weight vs RPM for Different Configurations	4-17
4-5	Configuration Lifting Capability at Constant RPM	4-18
4-6	Percentage of Lift for Various Test Configurations	4-19

ILLUSTRATIONS continued

FIGURE		PAGE
4-7	Inlet Fairing and Blower Wheel Have Been Moved Out of Cage to Show Relative Mounting Positions	4-24
4-8	Pressure Tests at Surface of Cage	4-28
4-9	Discharge Stack with Nylon Grid	4-30
4-10	Velocity Readings at Blower Inlet	4-31

TABLE

NUMBER		PAGE
3-1	Fan Characteristics	3-10
4-1	Load vs RPM Relationships for Test #1 (Quadruple Fan Installation)	4-4
4-2	Unit Area Pressures vs RPM for Test #1	4-7
4-3	Load vs RPM Relationships for Test #2 (Two Blower Wheel Installation)	4-11
4-4	Unit Area Pressures vs RPM for Test #2	4-12
4-5	Load vs RPM and Unit Pressure Relationships for Test #3	4-14
4-6	Percentage of Lift for Various Test Configurations	4-20
4-7	Load vs RPM and Unit Pressure Relationships for Test #4	4-22
4-8	Load vs RPM and Unit Pressure Relationships for Test #5	4-23
4-9	Load vs RPM and Unit Pressure Relationships for Test #6	4-27
4-10	Pressure Readings on Grid of Air Stack	4-32

SECTION 1

INTRODUCTION

25X1A

Prior to the innovation by the [REDACTED] of the air and liquid bearing concept, all commercial photographic film processing units transported film through the various sections and processing tanks on a series of rollers. These machines to which the term "conventional" may be applied, required a preponderance of driven rollers, each of which required rotation at precisely the same speed as all other rollers. Failure to achieve this synchronization of roller rpm could result in the formation of slack loops, abrasion, stretching or breakage of the film. The liquid and air bearing principle was a significant advance in the state-of-the-art. By providing a fluid or air cushion, in place of rollers, the film could literally be floated through the complete processing cycle with a minimum of mechanical contact with the machine.

This assignment was raised to determine if a bearing which incorporated an energy source as an integral part of the bearing would provide greater overall mechanical efficiency than a pressure plenum type, into which air is pumped from a remote blower.

SECTION 2

SUMMARY OF PRECEDING STUDY PROGRAM

2.1 SELF-POWERED AIR BEARING

As an extension of the work being carried out on a plenum-type bearing, a design study was made for a self-powered air bearing in which a fan would be incorporated to generate the air pressure and flow necessary to provide a transport cushion.

The use of a standard centrifugal blower, squirrel-cage wheel as a built-in power source presents difficulty because, to obtain optimum efficiency at the given design speed, the width of the wheel should not generally exceed 0.6 of the diameter. Various methods of avoiding this restriction can be employed, such as the use of two wheels, but achieving even flow becomes a serious problem over the length of the 9-1/2-inch bearing required. A mockup model of a bearing for a single film width of 70mm was constructed and provided a reasonable cushion after suitable flow restrictors had been provided to even the flow over the upper 180 degree half of the model, an intensive study was made of all available types of blowers. (See Monthly Progress Report No. 6, (Contract No. 974).

A new type of fan developed in Europe, the transverse-flow fan, showed promise for this application. A conventional centrifugal blower draws in air axially and discharges it outward radially through a different section of the fan periphery.

The advantage of incorporating this type of fan in an air bearing is that higher static pressures are obtainable for the same rotor diameter (a pressure coefficient of 1.8 to 5.5 as against 0.60 to 1.10) over a length restricted only by structural considerations, such as

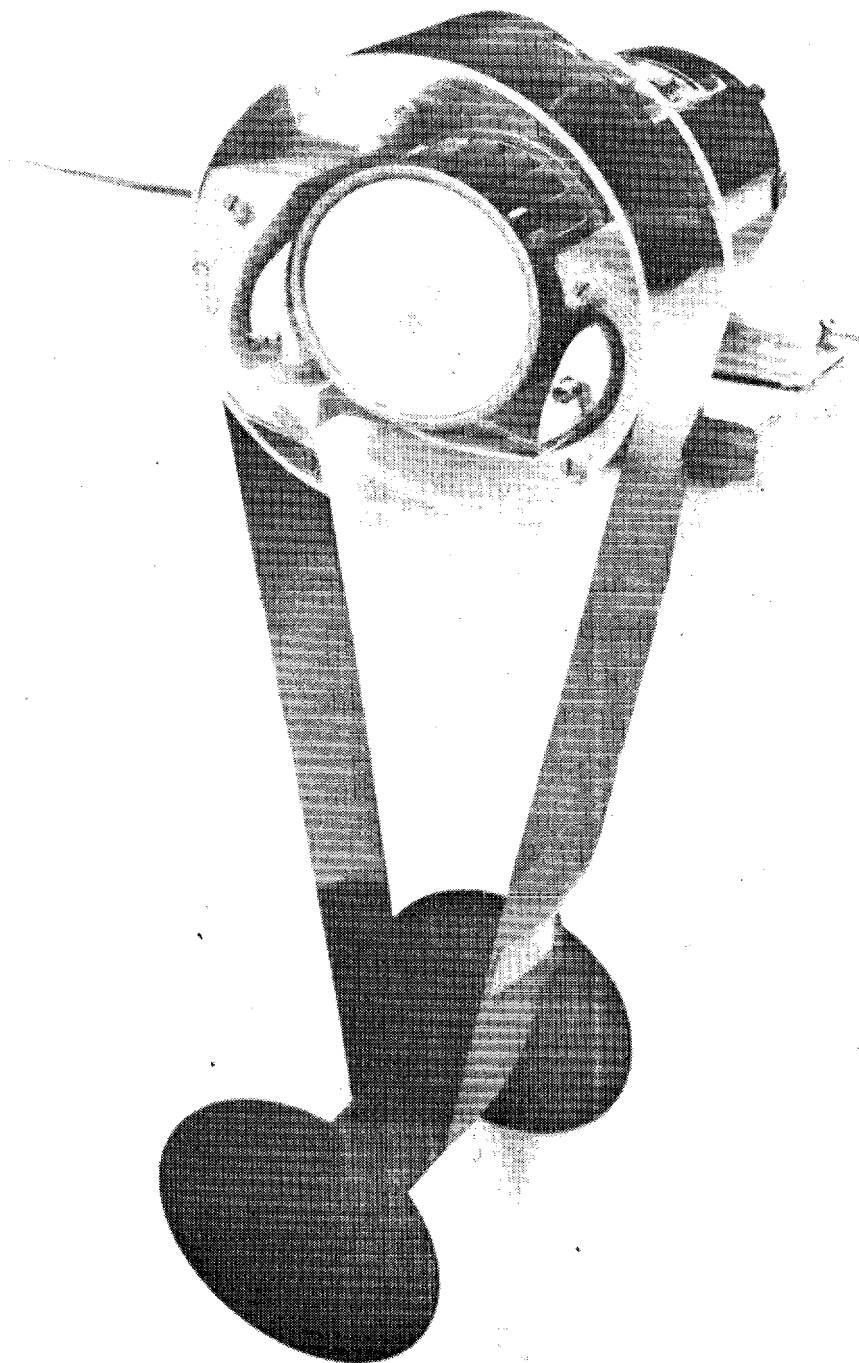


Figure 2-1. Air Bearing Using Transverse-Flow Fan

housing strength. A second mockup bearing, using an available wheel 1.8 inches wide, confirmed the feasibility of this concept (See Figure 2-1). The main problem appeared to be the air flow distribution over the required 9-1/2-inch length, which was hoped to be solved by using the transverse-flow fan.

The transverse-flow type fan selected was the Coester type in which two vortex generators cause a flow of air radially through the fan when the wheel is rotated. This type was selected since the drawing of air in through the lower half of the bearing and expelling it through the upper half best suited an air bearing configuration. The licensee of this design in the U.S.A. [REDACTED] cooperated to develop this concept, but unfortunately problems arose in this company's development program. It was found that a sudden transient obstruction in the output air flow could cause a reversal of flow in the vortex generators and therefore in the fan itself. In terms of an air bearing, this would cause the film to be drawn into the bearing.

25X1A

A further design concept was proposed by the [REDACTED] in which a Datwyler type of transverse-flow fan was integrated. However, this investigation was not pursued because of the air intake section being adjacent to one side of the film loop (See Figure 2-2).

25X1A

As an alternative to utilizing the transverse-fan concept, an experimental test stand was constructed (Figure 2-3) to determine whether a combination of propellers and fans could be utilized. Parts required at the time of this report are illustrated. (Figures 2-4, 2-5 and 2-6).

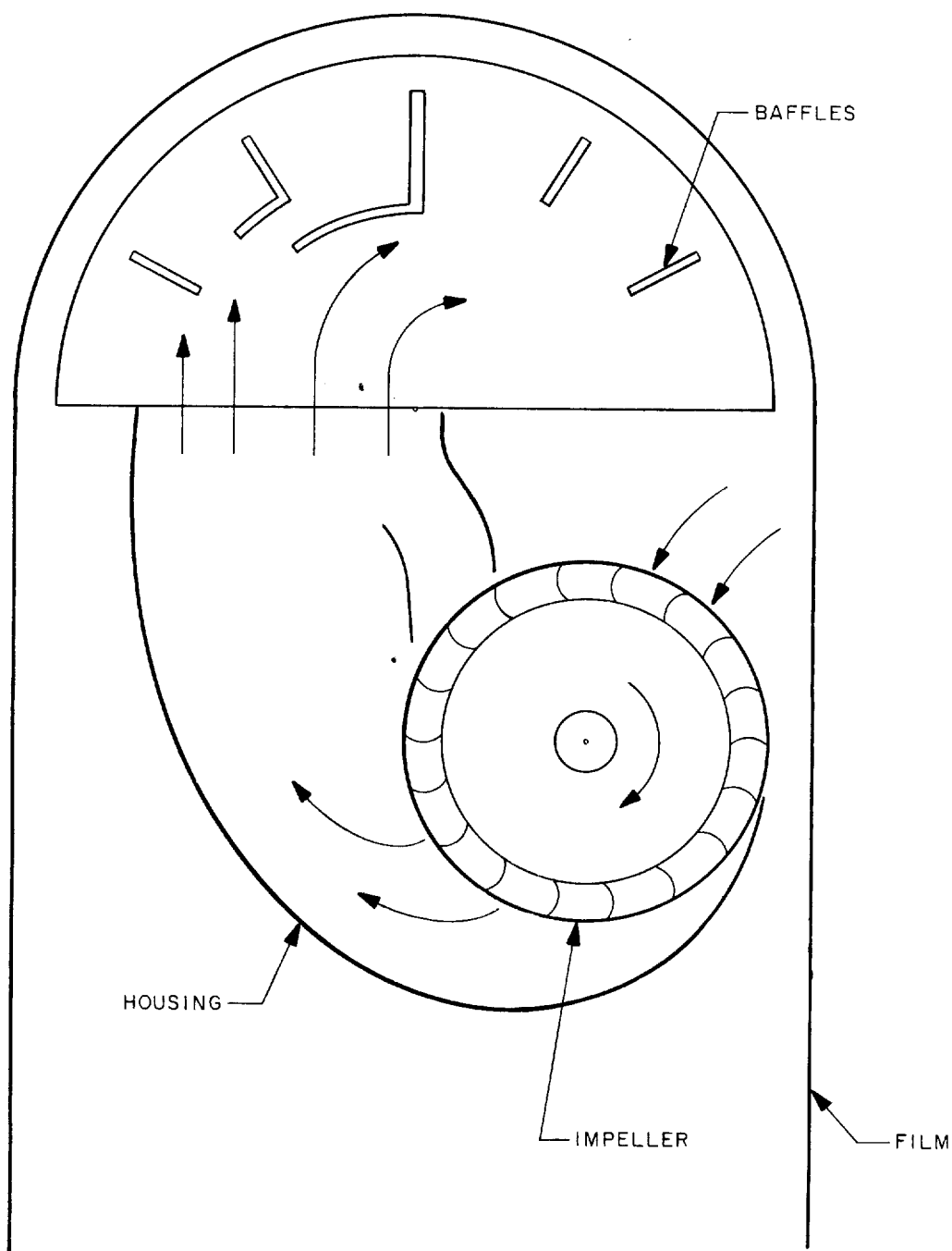


Figure 2-2. Scheme of Air Bearing with Transverse-Flow Fan

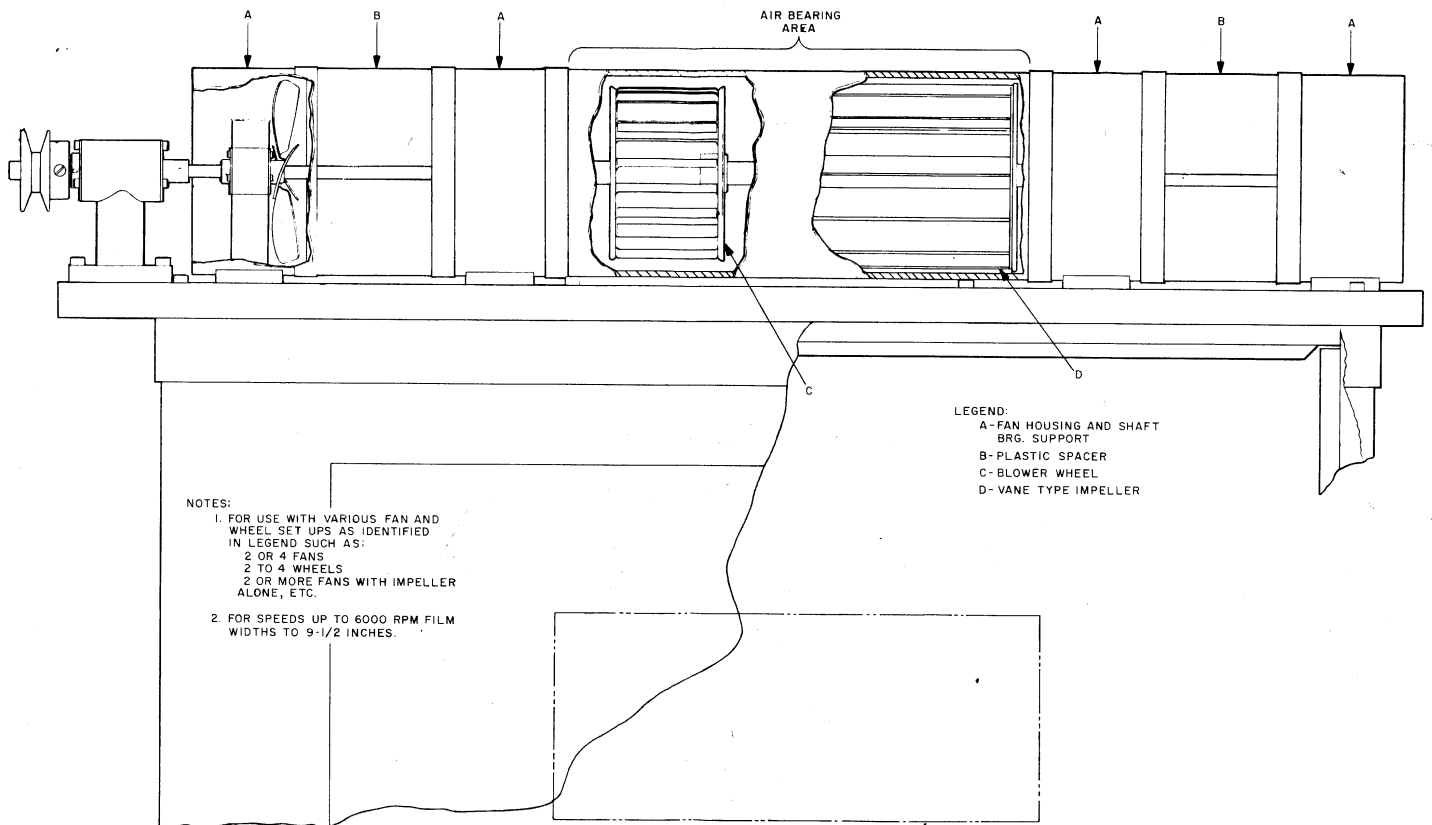


Figure 2-3. Layout of Air Bearing Test Bed

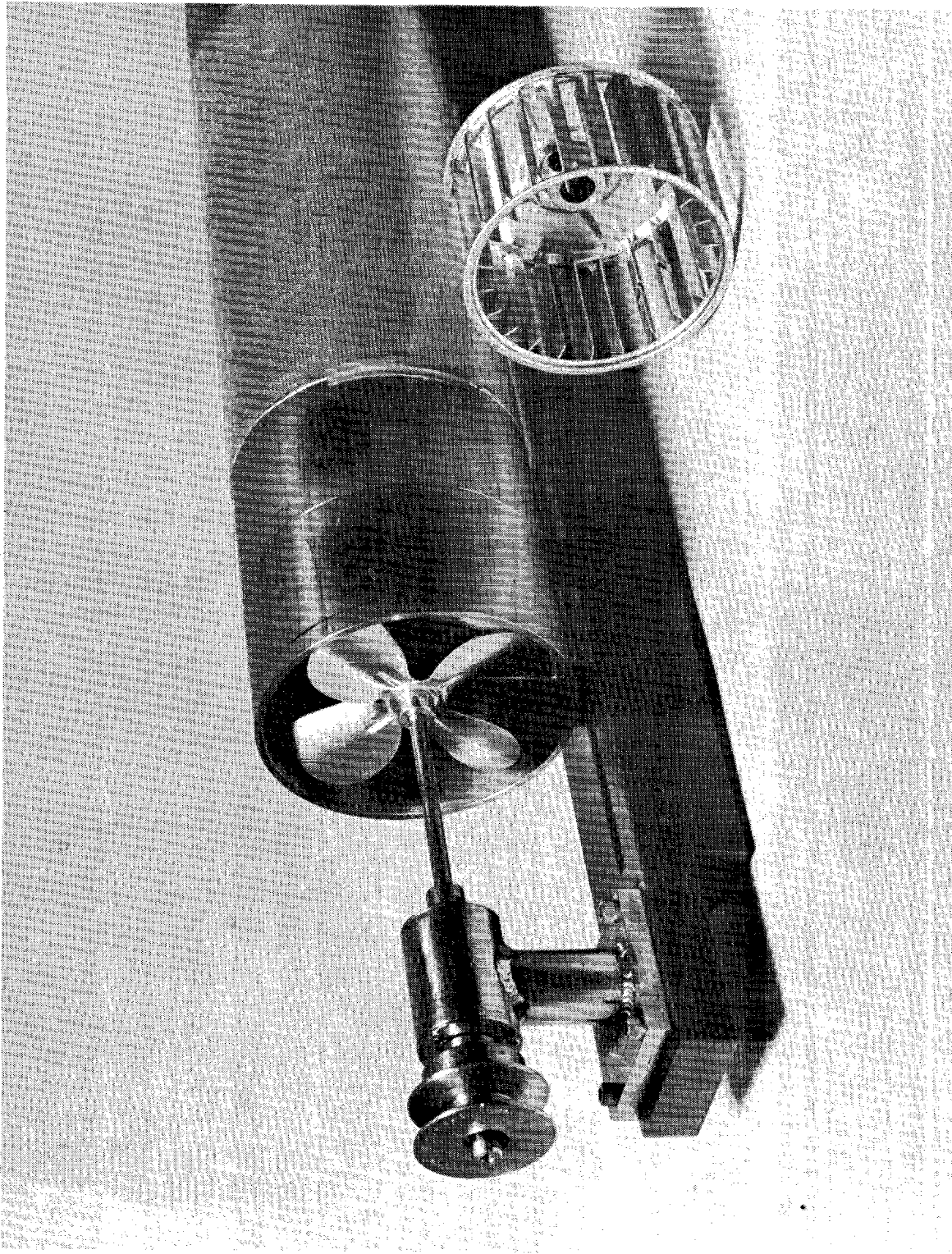


Figure 2-4. Air Bearing Test Bed Showing Fan Installed and Wheel

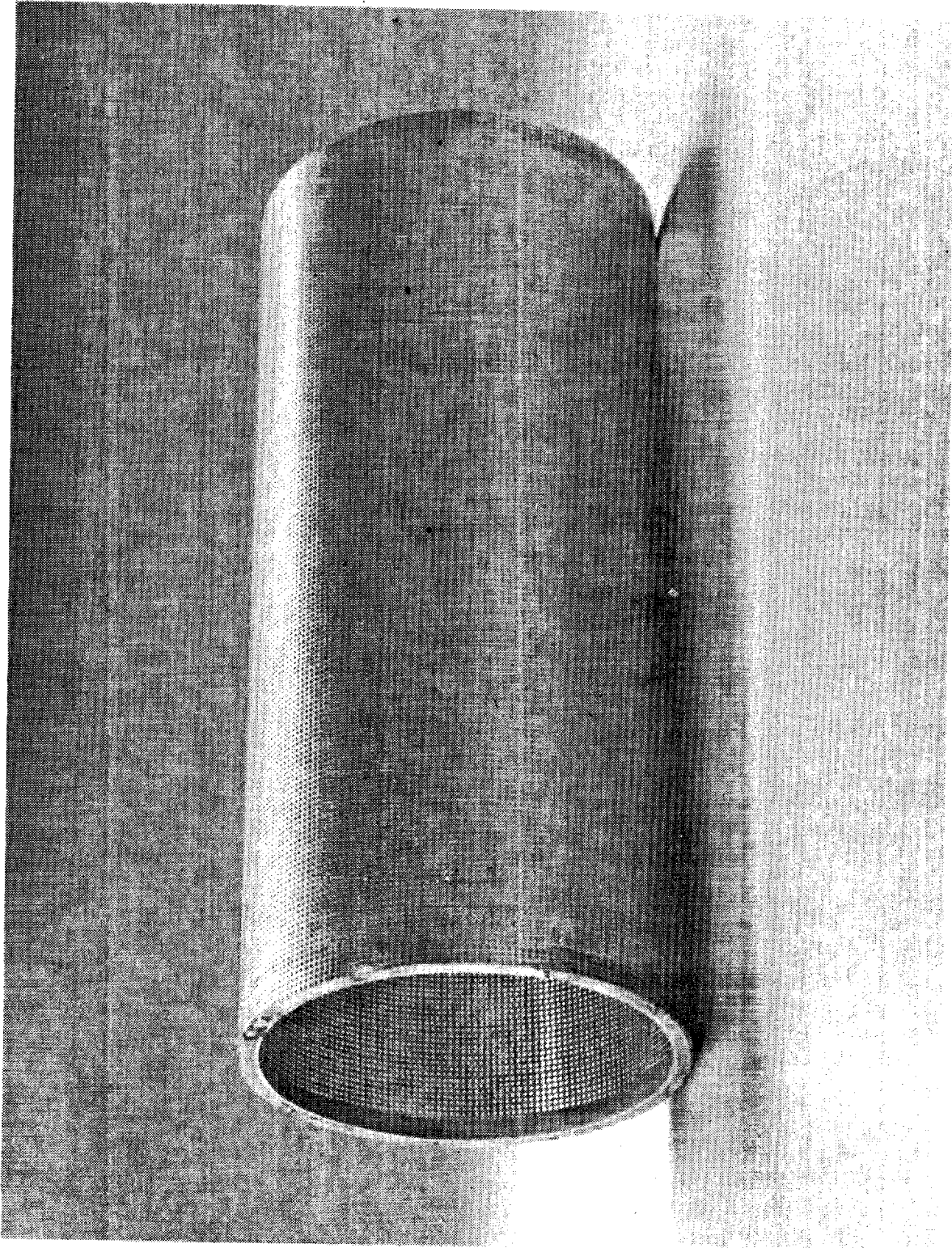


Figure 2-5. Perforated Cage

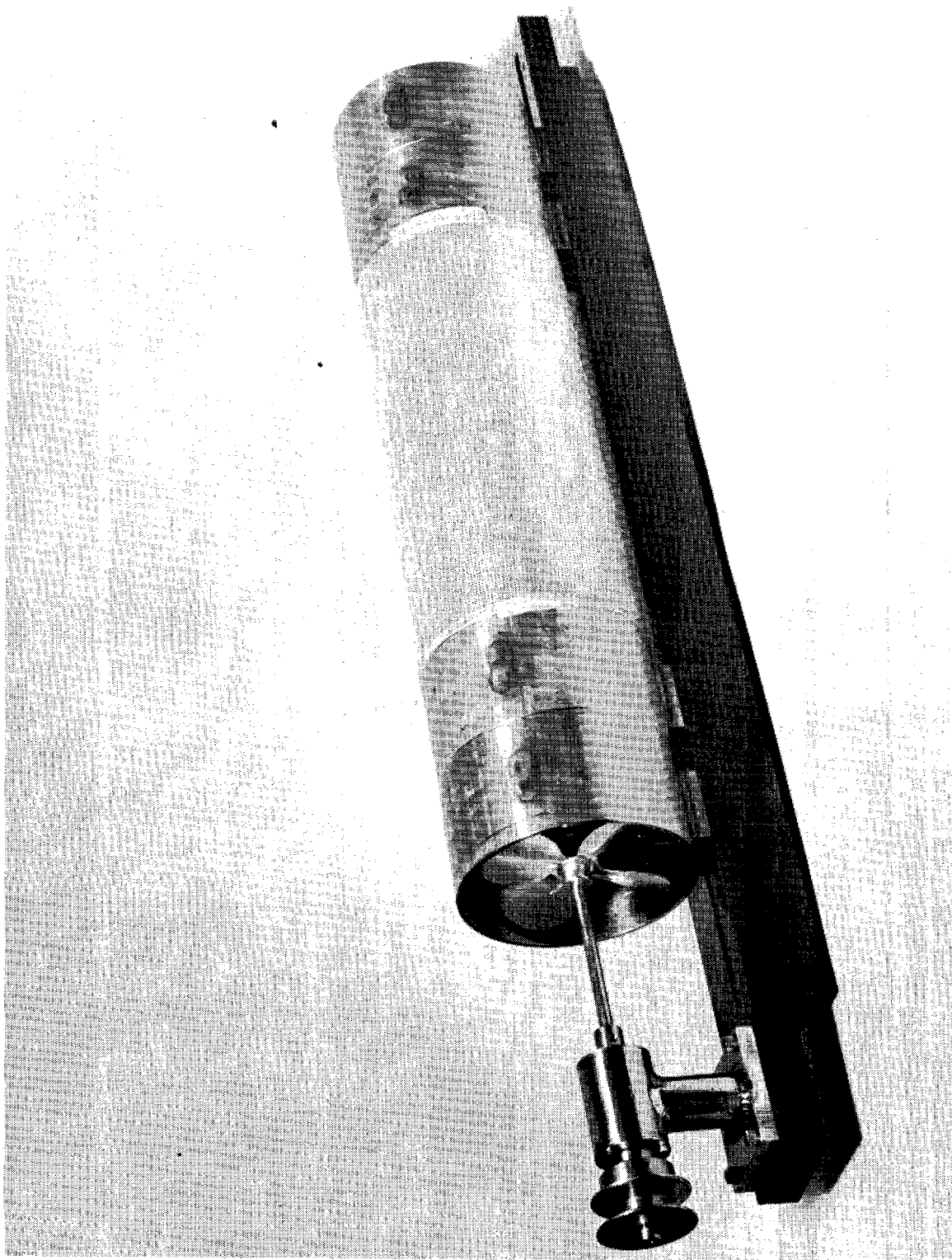


Figure 2-6. Air Bearing Test Bed Showing Fan Installation

SECTION 3

CONTINUATION OF STUDY PROGRAM

In this phase of the program the air bearing test bed was assembled, and various types and combinations of power generators (air accelerators) tested. The prime objective of the program was to determine the most efficient method of generating and sustaining a support cushion within the design concept of a bearing incorporating its own air source.

3.1 TECHNICAL DISCUSSION

3.1.1 Comparison of Liquid and Air Bearing Performance.

The theoretical performance of an air bearing follows the same laws as that of a liquid bearing. Changes in functional characteristics are caused by the immense differences between the viscosity and density of liquids as apposed to those of air. The compressibility factor of the gaseous media of an air bearing also causes significant fluctuations in the stability of the film loop over the bearing, dependent upon the operating pressures employed.

3.1.2 Air Bearing Test Bed.

The air bearing test bed was designed to permit the maximum number of flow and wheel combinations to be employed. It consisted of four-4-1/2-inch diameter shells in which a shaft bearing support was provided. Two of each of these shells were located at each end of a test bed, and were adjustable as to the distance between each (Figure 2-3). At one end of the test bed a fixed shaft bearing stand with a pulley mounting is located (Figure 2-4). The center area over which the film

was supported, consisted of a 4-1/2-inch diameter cylinder or cage 10-5/8-inches long, constructed of aluminum sheet, 0.027-inches thick, perforated with 0.041 diameter holes constituting approximately 29.7 percent of the bearing cage surface area (Figure 2-5). The seam joint was spot welded and was assembled on the undersurface (6 o'clock station) of the bearing, to minimize the effect of the weld. The 4-1/2-inch diameter was selected to suit standard commercially available fans and blower shells, and also to minimize bending loads of the film over the bearing.* The test bed was mounted on the top edge of the "Rotatron" liquid bearing test tank, and utilized the existing drive system, except for pulley diameter changes required to obtain the higher rpm needed for the air bearing performance (Figure 3-1).

3.1.3 Power Generators.

Within the test stand shells and cage, various combinations of fans (propellers) and centrifugal wheels were considered as offering the best performance output of a relatively low pressure per unit area, with high flow in cubic feet per minute. The generators used consisted of the following:

- 25X1A 1. Four-bladed, 4-inch diameter fans with a maximum allowable speed of 6200 rpm [REDACTED] Performance curves for these are given in Figure 8.

25X1A *Reference [REDACTED] "Determining the Force Required to Bend Film."

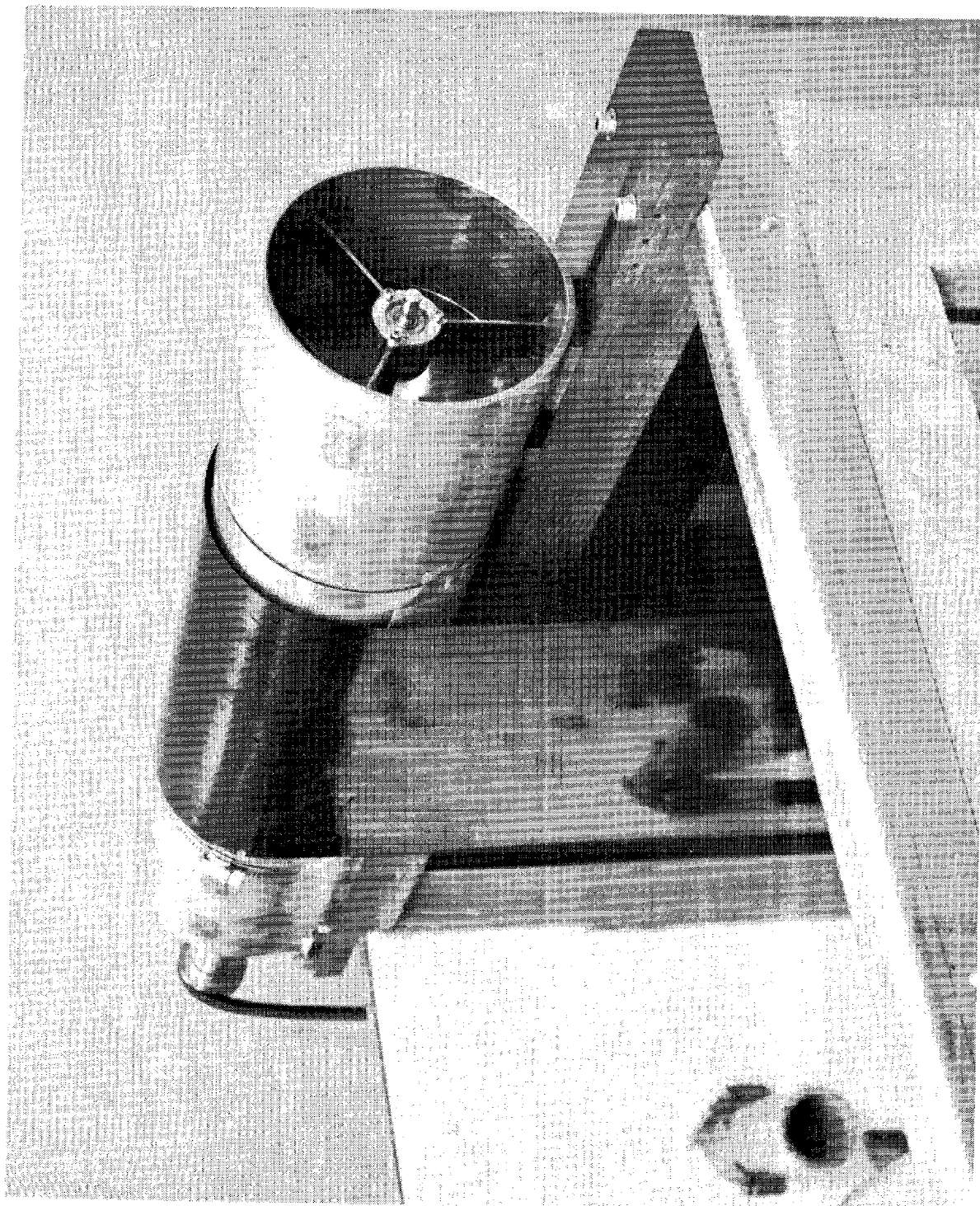


Figure 3-1. Bearing on Test Tank

2. Forward curved-blade type blower wheels 3.81-inches diameter,
2.5-inches long, with a maximum allowable speed of 6000 rpm

25X1A

[REDACTED]. Performance curves for these are given
in Figure 9.

3. Forward curved-blade type blower wheels, 2.50-inches diameter
and 0.97-inches long [REDACTED]. Performance
curves for these are given in Figure 10.

25X1A

3.1.4 Performance Data.

The performance data given by the curves for the power generators used in the test bed, were obtained from test chambers of a type provided by the equipment manufacturers to meet various codes, such as those of the National Association of Fan Manufacturers, Publication FM1-1955 of the National Electric Manufacturers Association, and by Bulletin 210 of the Air Moving and Conditioning Association. The performance curves for the fans and wheels used in this program have been included for reference purposes (Figures 3-2, 3-3 and 3-4) since they represent performances obtained under ideal conditions with casings or shrouds specifically designed for them, and although they are not directly applicable to the present configuration, still may be used for performance comparisons.

3.1.5 System Characteristics.

The resistance imposed against air flowing through any given air-circuit or system is commonly expressed as a pressure drop (ΔP) through the system. For any given (constant) system, ΔP will vary directly with the square of the air flow (velocity) through the system. Or, expressed by

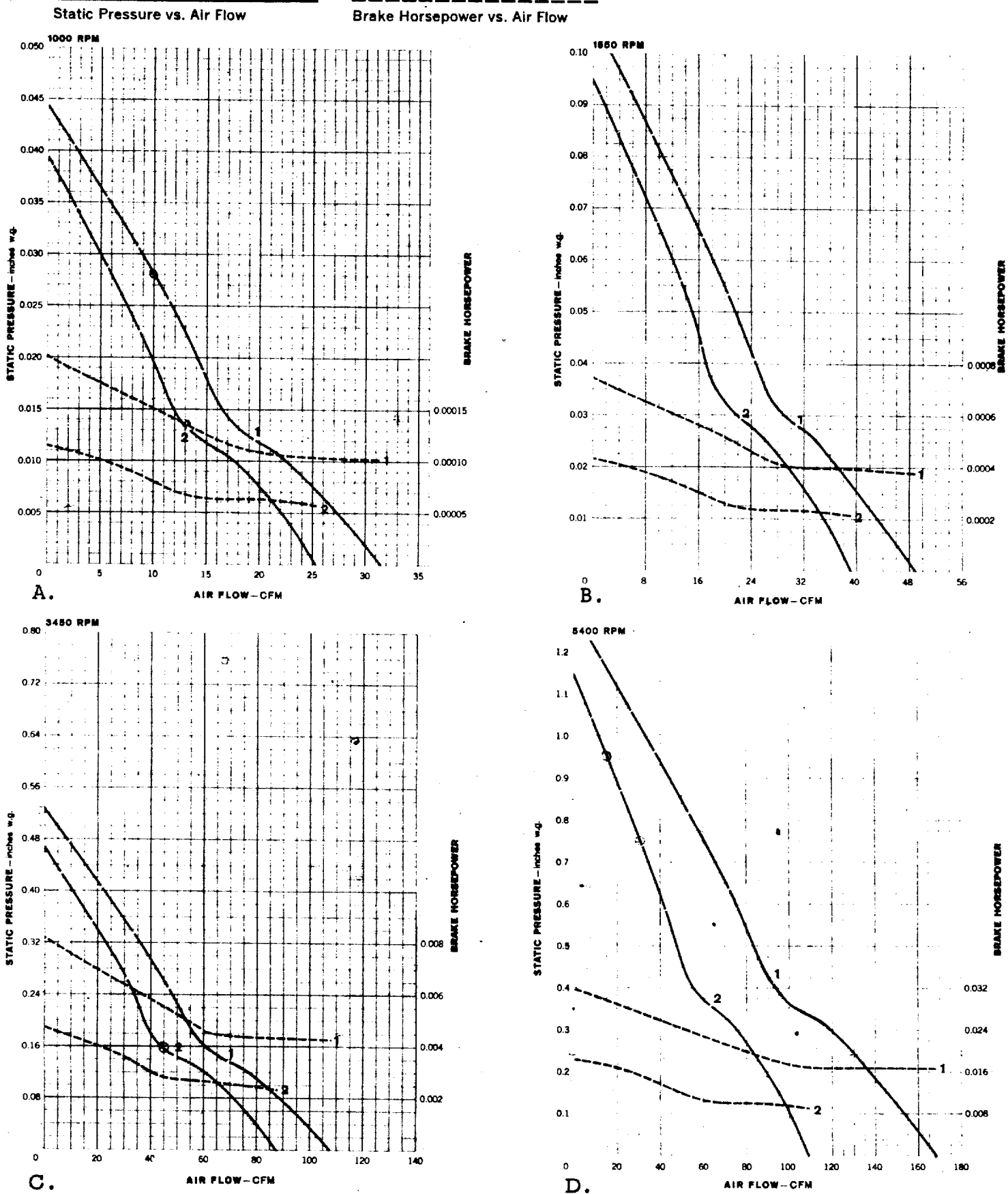


Figure A Performance Curves of Four-Bladed, 4-Inch Diameter Fans

25X1A

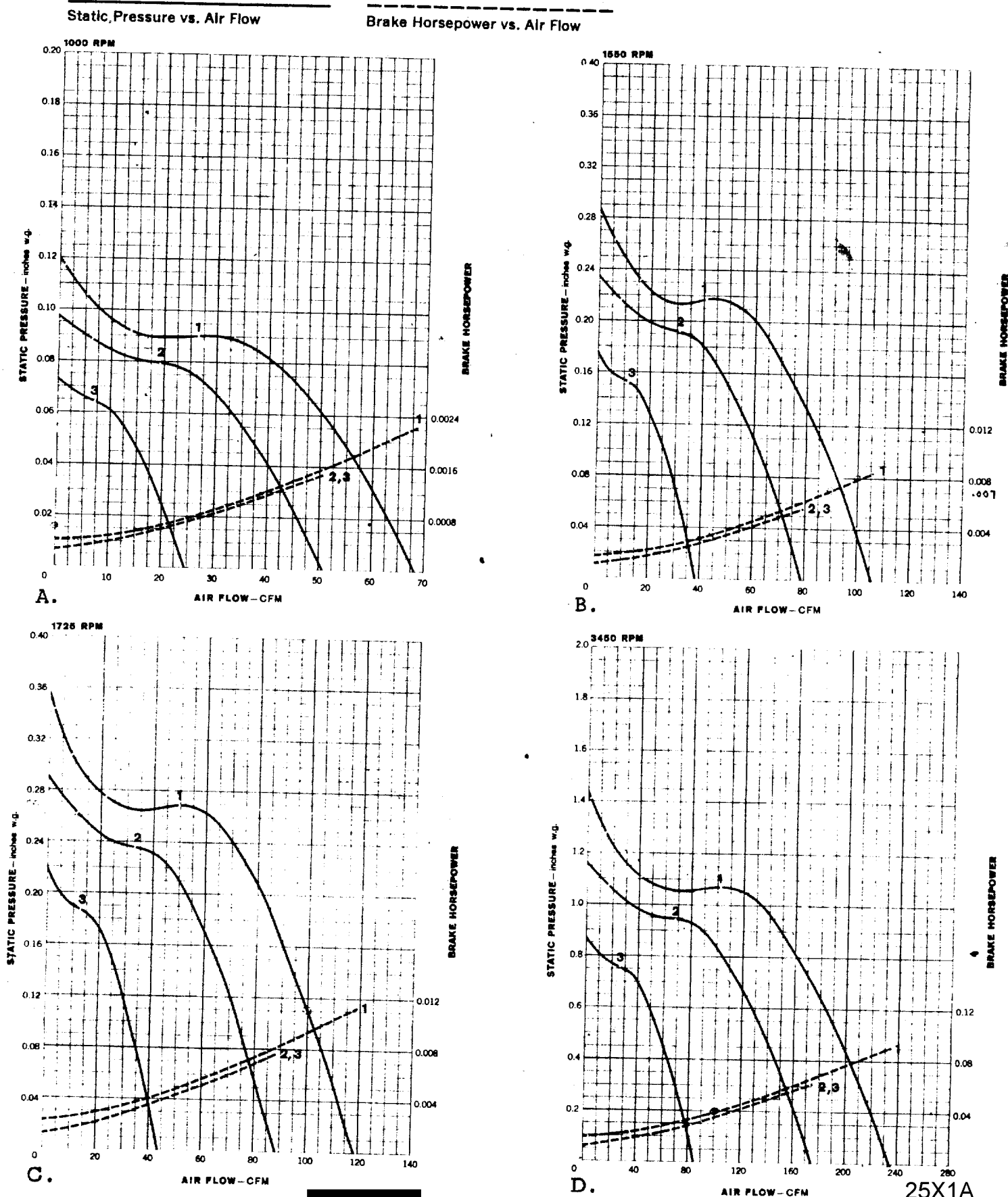


Figure 3-3. Performance Curves of

17 : CIA-RDP78B04747A002800060001-5

Forward-Curved, 3.81-Inch Diameter Blower Wheels

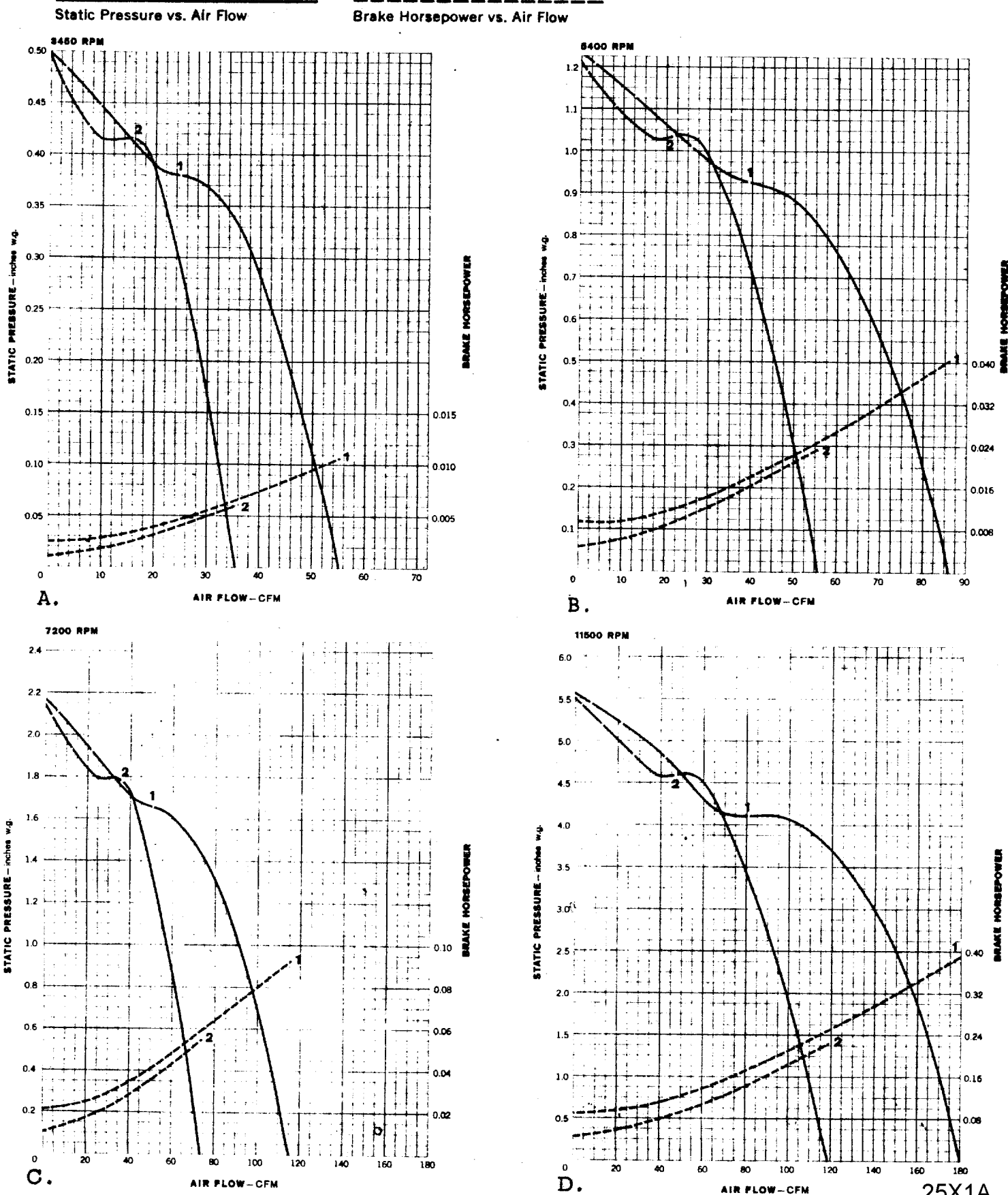


Figure 3-4. Performance Curves of [REDACTED] For [REDACTED] 25X1A
Approved For Release 2000/04/17 : CIA-RDP78B04747A002800060001-5

the generalized Bernoulli conservation of energy equation:

$$E = h + \frac{V^2}{2g} \quad \text{ft-lb/lb} \quad (3-1)$$

Where E is the total energy of the gas in motion, h its enthalpy and its velocity, V, squared over gravity represents its kinetic energy. The kinetic energy of the system can be considered unchanged from the entrance to the discharge areas of the blower since the hydrodynamic energy lost from the stream is converted into heat and returned to the gas in this form.

It would appear, with only cursory examination, that the ratio of the total available supporting surface area of the air bearing to the area of film supported (and consequently the lifting capacity in unit weight per square inch) would be a direct, or straight line, relationship. Expressed in another way, a five-inch wide film should be able to support one half the weight of a ten-inch film (i.e. same unit area loading), all other factors being equal, depth of cushion, rpm, configuration, etc. This assumption, however, is not valid. While, in both cases, the air escapement plenum on either side of the annular area of film cushion is identical, for narrower films, the larger exposed area of the bearing surface permits a greater pressure drop and reduces the supporting cushion's weight bearing capability. The complex relationship can be seen to be more nearly geometric than arithmetic. This phenomenon accounts, in a large measure, for the recorded eccentricities in bearing performance with various widths of film and with rpm constant.

System Characteristics can be conveniently approximated by the use of

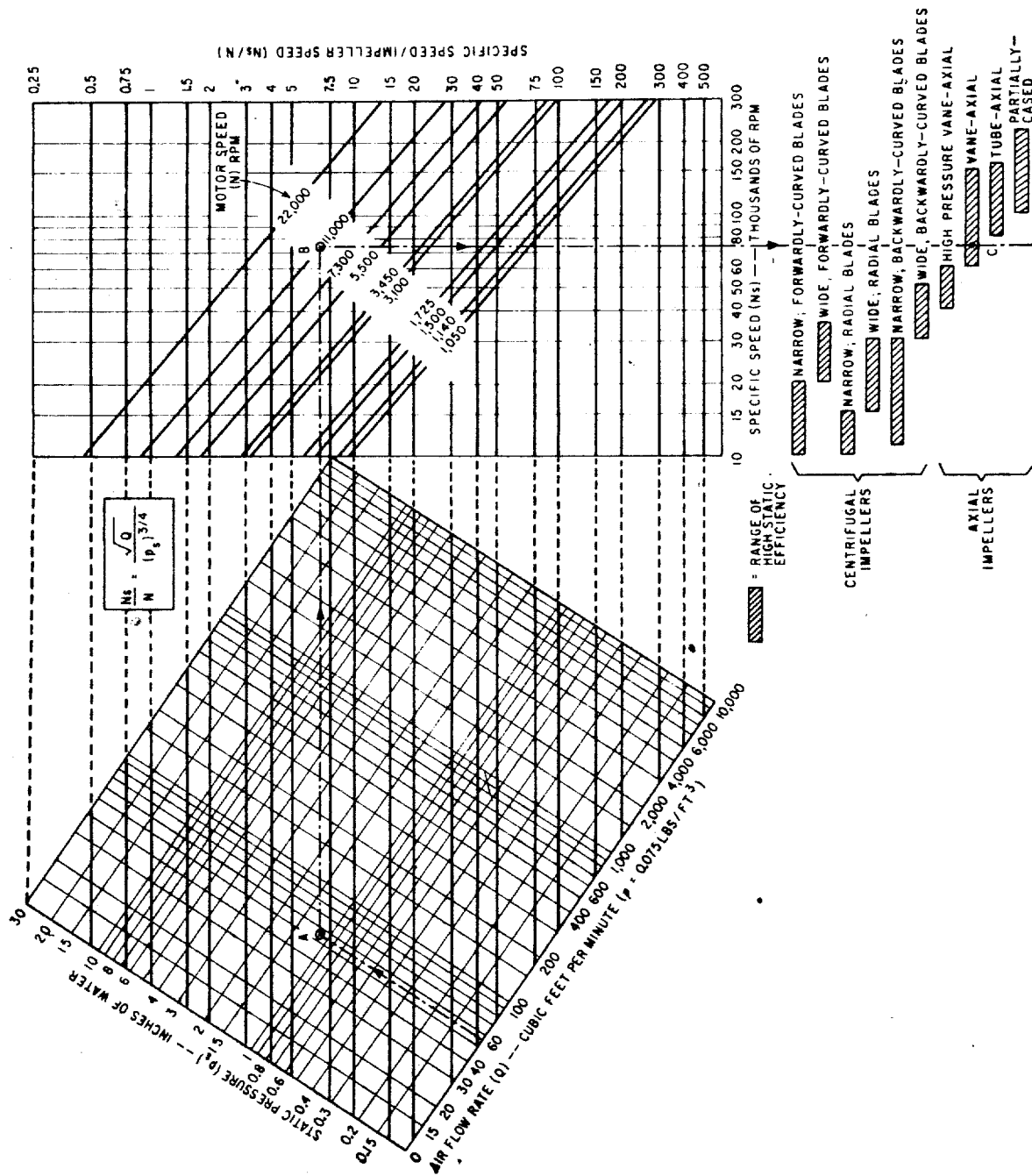

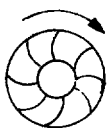
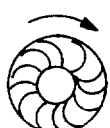


Figure 3-5. Graph for Determining Type of Fan for a Specific Application

Table 3-1 and Figure 3-5. Figure 3-5 can be used to determine static pressures for different air flows and rpm's. The type of blade curvature is critical in centrifugal (or "squirrel-cage") impellers (no one type being clearly superior to the others) since peak efficiencies are a function both of type and speed. The optimum choice, in this case, is obviously one whose peak encompasses static pressures sufficient to support all widths of film (from 70mm to 9-1/2-inch) without format changes.

A characteristic of this type of blower wheel is the higher output (Pv) at the back face (opposite intake ends) of the impeller. Because of this ram effect of the incoming air stream, these types of impellers are usually 0.5 to 0.6 of their diameter in length, drag losses being greater than the output gain for greater lengths. Even so, the higher Pv at the inside end is considerable.

TABLE 3-1 FAN CHARACTERISTICS

Type	Blade Design	Name	Pressure Coefficient ψ^*
Centrifugal		Forward-Curved	1.0 to 2.0
		Radial-Bladed	1.0 to 1.4
		Backward-Curved	0.60 to 1.10

*Where the following relationship obtains:

$$D = \frac{1.53 \times 10^4}{N} \sqrt{\frac{P_s}{\psi}}$$

D = Diameter of fan in inches

N = RPM

P_s = Static pressure in inches of water

3.1.6 Principal System Elements.

The research program centered on a quadruple unit employing two different diameters and lengths of forward-curved blowers mainly because time and budget did not permit optimizing the design with ideal prototypes. Theoretical considerations are presented subsequently in this report. Other configurations in this research series embodied combinations of fully encased axial propeller-type impellers together with the centrifugal blowers. It was felt that, since the axial fans fully shrouded in the main plenum inlet were operating at maximum efficiency, they would supply sufficient movement of air to the intake area of the centrifugals. This, in turn, was expected to permit higher static pressures on the periphery of the perforated cage which performs the final transformation of kinetic energy.

3.1.6.1 Bearing Cage.

The perforated bearing cage was selected to provide a plenum chamber in which the kinetic energy could be (partially) transformed into pressure, the pressurized trapped air subsequently escaping through the perforations to provide the desired air cushion. Because these same perforations exist around the periphery of the blower wheel, a certain amount of the air is projected directly through the holes. This quantity of air still possesses unconverted kinetic energy (P_v).

SECTION 4

TEST PROGRAM

4.1. TEST #1. QUADRUPLE FAN INSTALLATION

The evaluation program was commenced with the installation of two 4-1/2-inch diameter, four-bladed radial fans in tandem, in each end of the test bed (Figure 4-1A). The fans were run at speeds of 4100, 5200 and 5800 rpm. Four widths of thin-base film, 70mm, 5.0-, 6.6- and 9-1/2-inches were loaded to produce an air bearing cushion 1/8-inch in height at each fan speed. The loads supported by the test bed with these film widths are given in Table 4-1.

The cushion of 1/8-inches height, was acceptable with regard to concentricity of the film loop about the bearing periphery, and to stability with the lower section of the cage closed between the 8 o'clock and 4 o'clock stations over the whole bearing length. No regular oscillation of the loop was observed. Reference to Table 4-1 shows that the maximum loads lifted, when converted to a dynamic load equivalent [REDACTED], "To Determine the Coefficient of Friction of Film") would be restrictive for use in a large processor involving a long film path and many air bearings, i. e. the cushion would collapse, or a restriction in processing speed would be necessary.

25X1A

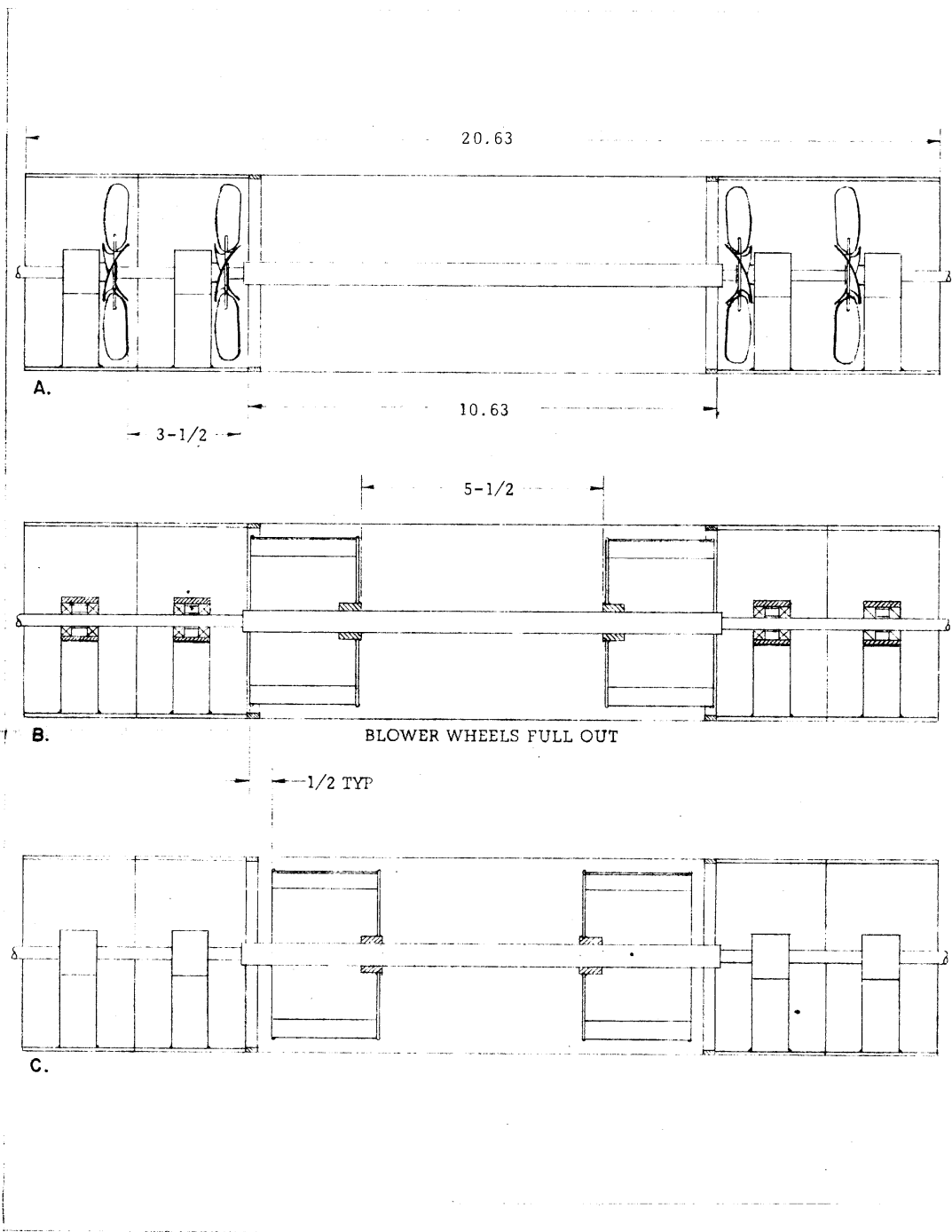


Figure 4-1. Test Bed Impeller Configurations

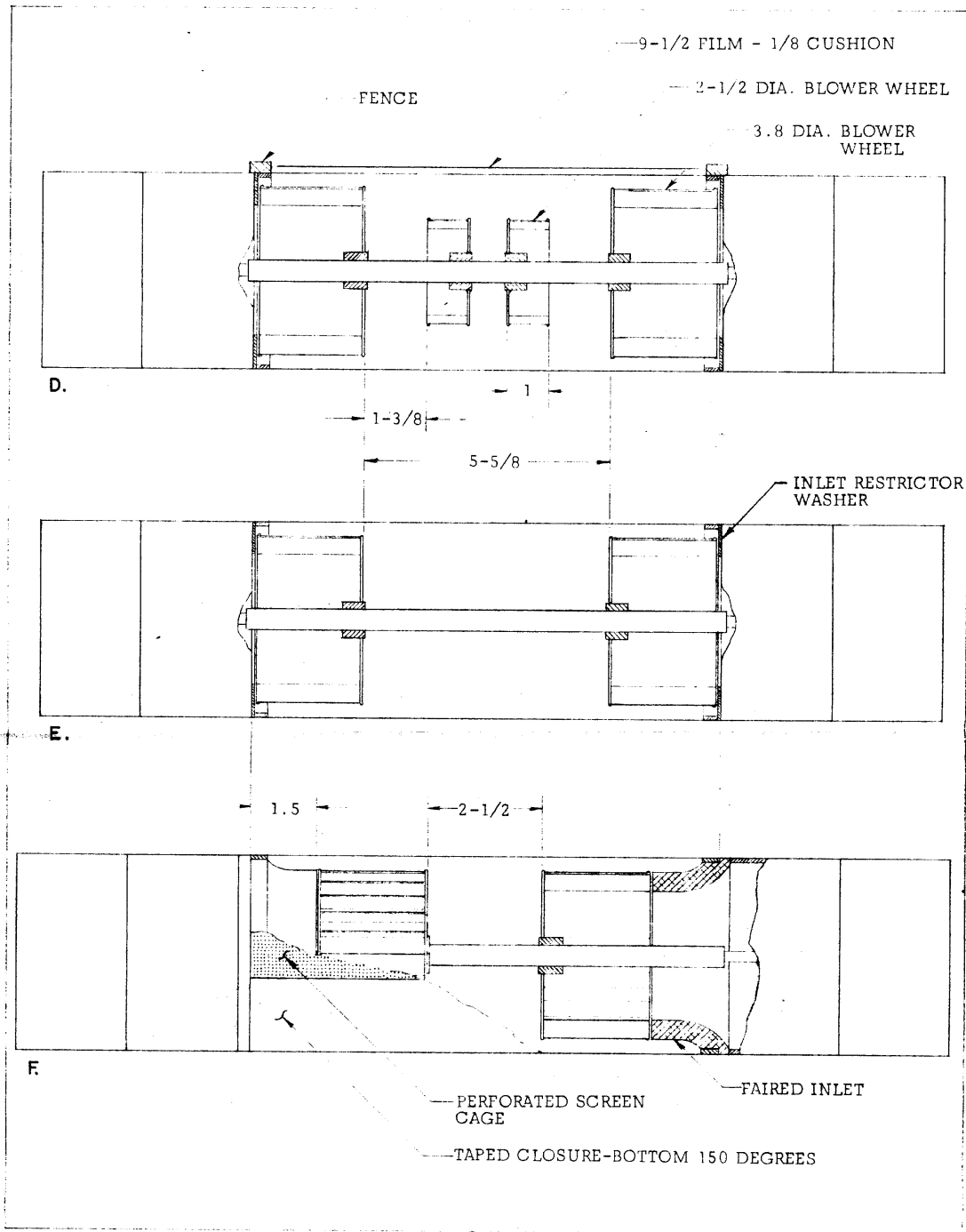


Figure 4-1 (Continued). Test Bed Impeller Configurations

TABLE 4-1

Load vs RPM. Relationships for Test #1
(Quadruple Fan Installation)

Film Width	Impeller Speed (rpm)	Cushion Height	Supported Load (lbs.)
9-1/2-Inch Film	4100	1/8-Inch for All	0.25
	5200		0.40
	5800		0.50
6.6-Inch Film	4100		0.10
	5200		0.16
	5800		0.20
5-Inch Film	4100		0.08
	5200		0.13
	5800		0.16
70mm Film	4100		0.03
	5200		0.05
	5800		0.06

A comparison can be made between film width, fan speed and load supported. In order to clarify the rationale used in calculating the bearings film supporting area, a brief review of the physics involved is in order. In Figure 4-2, if A is considered an end view of a typical

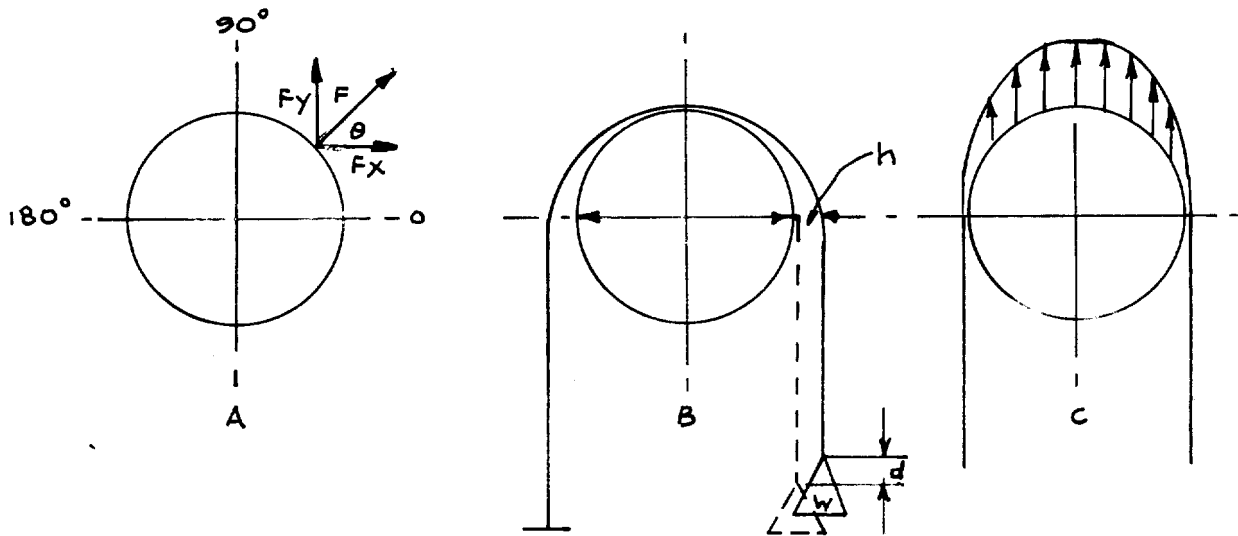


FIGURE 4-2. Bearing Support Characteristics

air bearing, any stream of air emerging from the plenum will leave the cage normal to the surface at that point (F in the diagram). The horizontal component of the force is seen to be F_x and the vertical F_y . Only the vertical component (expressed by $F \sin \theta$) contributes to lift, the y -component holds the film away from the bearing surface. Reference to diagram B. shows that if only the horizontal component were in effect, such a force would produce a cushion, h , at the 0 and 180-degree positions. In so doing, it would raise the load, W , some finite increment, d . The work performed in the case would be Wd , but it must be noted that this does not contribute to lifting the film at the 90-degree

position. If the lifting forces were integrated from zero to 180-degrees (Figure 4-2C), only the projected plane of the film would be involved in the $F \sin \theta$ summation. With this in mind, calculations of the bearing area of each width of film, with a 1/8-inch cushion throughout, can be made.

These become:

9-1/2-inch	-	45 sq. in.
6.6-inch	-	31 sq. in.
5.0-inch	-	27 sq. in.
70m/m	-	13 sq. in.

By dividing the bearing area of the film loop, into the load lifted by the particular film width, the values in Table 4-2 representing the unit area pressure, are obtained.

TABLE 4-2.

Unit Area Pressures vs RPM for Test #1

Film Width	Impeller Speed (rpm)	P. S. I.	Unit Area Pressure
			Ins. W. G.
9-1/2-inch	4100	0.00556	0.154
	5200	0.00889	0.246
	5800	0.01112	0.308
6.6-inch	4100	0.00323	0.0894
	5200	0.00517	0.143
	5800	0.00645	0.179
5-inch	4100	0.00296	0.0822
	5200	0.00482	0.1335
	5800	0.00593	0.1640
70m/m	4100	0.00231	0.064
	5200	0.00385	0.1065
	5800	0.00462	0.128

It will be noted that, for example, with 70m/m film, with an operating speed of 5800 rpm, a lower unit area support pressure is produced than with the 9-1/2-inch film under the same operating conditions. This observation serves to illustrate a basic problem in the design of an air bearing, namely that a pressure and flow satisfactory for the support of a 9-1/2-inch film cannot be assumed to be satisfactory for a narrower film. With the narrower film, a greater area of the cage is exposed, which decreases the pressure and increases the flow out of this area. A decrease in the unit area support pressure under the film loop is thereby caused, or $P_v = \frac{(V)^2}{(4005)}$ (4-1)

where:

P_v = velocity pressure (inches water)

V = velocity of flow (fpm)

The factor, 4005, takes account of the density of air and gravitational forces.

In pressure-plenum type air bearings, with a fixed power source, the method used to overcome this, is to install format changers which close the slots or holes in the open areas, and also provide edge barriers to restrict the flow out of each end of the film loop.

4.1.1. Efficiency of Configuration.

With no film loop present, a flow reading taken at the bearing intakes approximated 140 CFM. With pressure varying as the square of the velocity, and using the idealized performance curves in Figure 3-2 D

for the 5400 rpm impeller speed, the following performance estimates can be made. Average static pressure head for all film widths at

4100 rpm is 0.0974 ins. W.G.

5200 rpm is 0.1573 ins. W.G. (Reference
Table 4-2)

5800 rpm is 0.1947 ins. W.G.

average static pressure head for all film widths at

$$5400 \text{ rpm is } \left(\frac{5400}{5800} \right)^2 \times 0.1947$$

which is 0.169-ins. W.G. Reference to the performance curve shows a CFM of approximately 95. Since the fans are in tandem and the average pressure is the product of these at each intake end, the total CFM is $95 \times 2 = 190$ total CFM (with no system pressure losses). The efficiency of the fans in this configuration can therefore be approximated as

$$\frac{\text{Measured CFM}}{\text{Theoretical CFM}} \times 100 = \quad (4-2)$$

$$\frac{140}{149} \times 100 = 93.7 \text{ percent} \quad (4-3)$$

4.2 BLOWER WHEEL INSTALLATIONS

4.2.1. TEST #2 TWIN 3.81 - INCH DIAMETER BLOWER WHEELS

Position 1

In this test, two blower wheels were installed in the test bed, with the open end of the wheels facing the open ends of the test bed, and level with the end of the bearing cage. (Figure 4-1B). With this installation of blower wheels drawing air in axially through each end of the bearing, and discharging it radially through the wheels, it was anticipated that

higher pressure areas would result at each end of the cage, with a lower pressure area between the wheels due to the wheel diaphragms. One result of this would be revealed in undue edge fluttering of the film, or "dancing" of the film loop about the bearing. The impellers were run at 4150, 5200 and 5800 rpm, with four film widths weighted to produce a cushion height of 1/8-inch. The results are shown in Table 4-3.

In the foregoing tests, an acceptably stable cushion was obtained with good concentricity of the film loop over the bearing. No edge flutter or undue dancing of the film loop was observed.

From the loads supported by the four widths of film, the unit area pressure can again be calculated for this configuration. The values are given in Table 4-4.

4.2.2. Efficiency of Configuration.

With no film loop present, as in the previous efficiency evaluation, a flow reading was taken of the bearing intakes and was recorded as 224 C.F.M.

The static pressure heads for all the film widths at each rpm was averaged and the following values obtained.

TABLE 4-3

Load vs RPM Relationships for Test #2
(Two Blower Wheel Installation)

Film Width	Impeller Speed (RPM)	Cushion Height	Supported Load (lbs.)
9-1/2-Inch	4150	1/8-Inch for All	0.44
	5200		0.68
	5800		0.86
6.6-Inch	4150		0.23
	5200		0.36
	5800		0.45
5.0-Inch	4150		0.14
	5200		0.22
	5800		0.27
70 m/m	4150		0.10
	5200		0.15
	5800		0.19

TABLE 4-4

Unit Area Pressures vs RPM for Test #2

Film Width	Impeller Speed (rpm)	<u>Unit Area Pressure</u>	
		P. S. I.	Inches-WG
9-1/2-inch	4150	.0098	0.271
	5200	.0151	0.418
	5800	.0191	0.528
6.6-inch	4150	.0074	0.205
	5200	.0116	0.321
	5800	.0145	0.401
5.0-inch	4150	.0052	0.144
	5200	.0082	0.227
	5800	.0100	0.277
70m/m	4150	.0077	0.213
	5200	.0115	0.319
	5800	.0146	0.404

4150 rpm	-	0.208 WG
5200 rpm	-	0.321 WG
5800 rpm	-	0.403 WG

In order to correlate the above values with the idealized wheel performance, it is necessary to obtain the average static pressure head at

$$3450 \text{ rpm. } \left(\frac{3450}{4150} \right)^2 \times 0.208\text{-inches WG} = 0.144\text{-inches WG.}$$

Reference to the performance curve on Figure 3-3D shows a CFM of approximately 235. Since a wheel is installed at each end of the bearing the total theoretical CFM would be $235 \times 2 = 470$ with no system losses. The efficiency of this configuration can therefore be approximated as

$$\frac{\text{Measured CFM}}{\text{Theoretical CFM}} \times 100 = \quad (4-4)$$

$$\frac{224}{470} \times 100 = 47.7 \text{ percent.} \quad (4-5)$$

4.3 TEST #3. TWIN 3.81-INCH DIAMETER BLOWER WHEELS

Position 2

To determine if a change in location of the two blower wheels would increase or decrease the bearing efficiency, tests were conducted with the blower wheels moved inboard by 1/2-inch from the cage ends (Figure 4-1C). The results are shown in Table 4-5. As in Test #2, the four widths of film were loaded to maintain a cushion of 1/8-inch.

TABLE 4-5

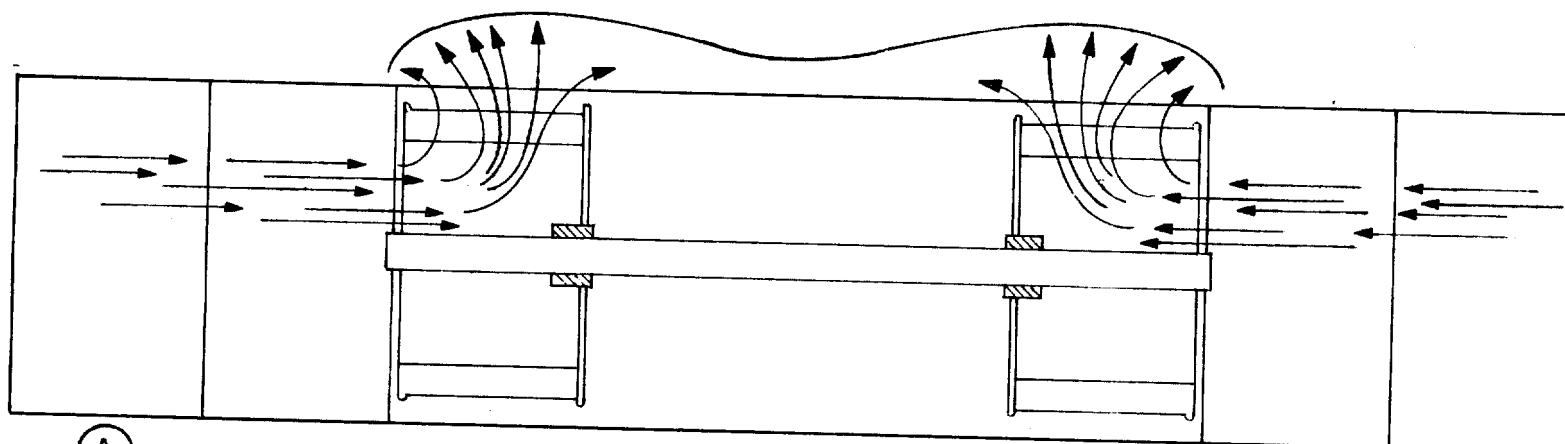
Load vs RPM and Unit Pressure Relationships for Test #3

Film Width	Impeller Speed (rpm)	Load Supported (lb)	Unit Area Pressure		Support Area (sq.inches)
			P. S. I.	Ins. WG	
9-1/2-inch	3450	0.54	.012	0.332	45
	4200	0.81	.018	0.499	
	5200	1.24	.028	0.776	
	5800	1.55	.034	0.943	
6.6-inch	3450	0.30	.0097	0.268	31
	4200	0.45	.015	0.416	
	5200	0.70	.023	0.637	
	5800	0.87	.028	0.775	
5.0-inch	3450	0.17	.0063	0.174	27
	4200	0.25	.0093	0.257	
	5200	0.35	.013	0.360	
	5800	0.48	.018	0.499	
70m/m	3450	0.08	.0062	0.172	13
	4200	0.12	.0092	0.255	
	5200	0.18	.014	0.388	
	5800	0.25	.019	0.527	

From the results obtained, some interesting comparisons can be drawn between Test #2 and Test #3. In the former test, the 9-1/2-inch film at 5800 rpm supported a load of 0.86 lb, while in Test #3, at the same impeller speed, a load of 1.55 lb was supported. In the latter case, however, while a satisfactorily concentric cushion was obtained, the 9-1/2-inch film showed a tendency to slide off the cushion "crown" (Figure 4-3B). Further movement of the wheels inboard towards the bearing center, while providing a greater Pv, also accentuated the cushion crown effect, resulting in an increased tendency for the narrower films also to slide off center (Figure 4-3C). The selected inward movement by 1/2-inch of the wheels therefore represented the best compromise between a maximum increase in the Pv value, for a minimum increase in instability of the film loop.

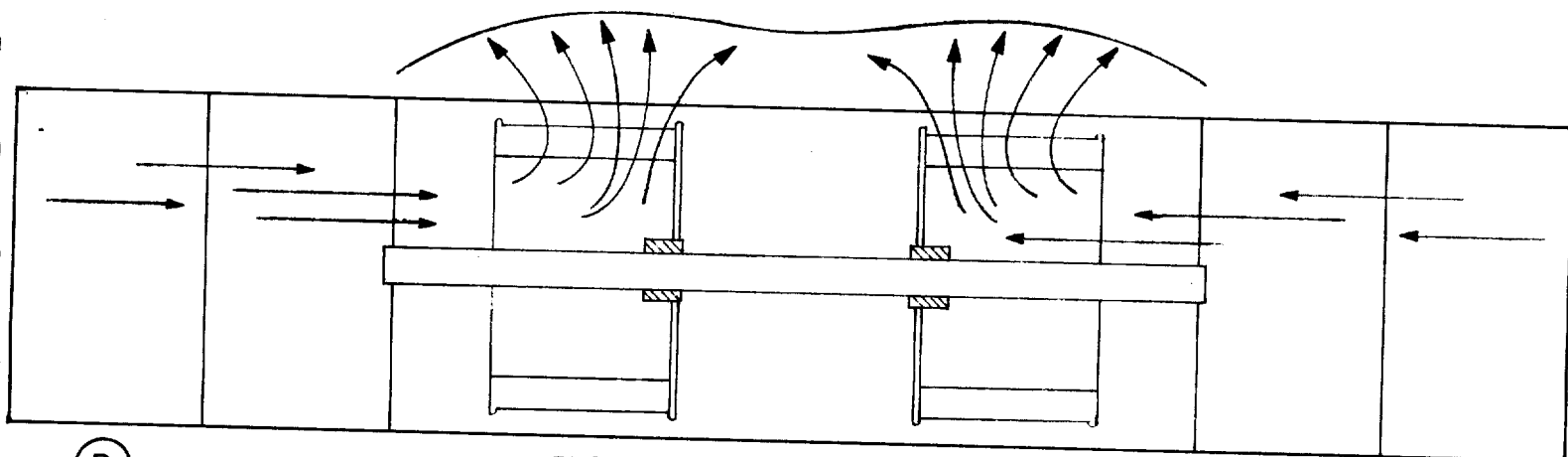
4.3.1. Efficiency of Configuration.

A comparison of efficiency between the configuration of Test #2 and this test (#3) configuration can be obtained from Figures 4-4, 4-5 and 4-6. Figure 4-4 shows a family of curves representing the loads lifted over the range of impeller speeds used in the tests for all film widths employed. From this chart, an extract was made of the loads supported at 5800 rpm for all film widths and converted into a table of percentages of the maximum load lifted for any film width. (Figure 4-6 and Table 4-6). From this table, the family of curves representing the percentage of maximum lift in each test configuration for each film was compiled. From these curves, it will be noted that the best lifting characteristic for 70m/m



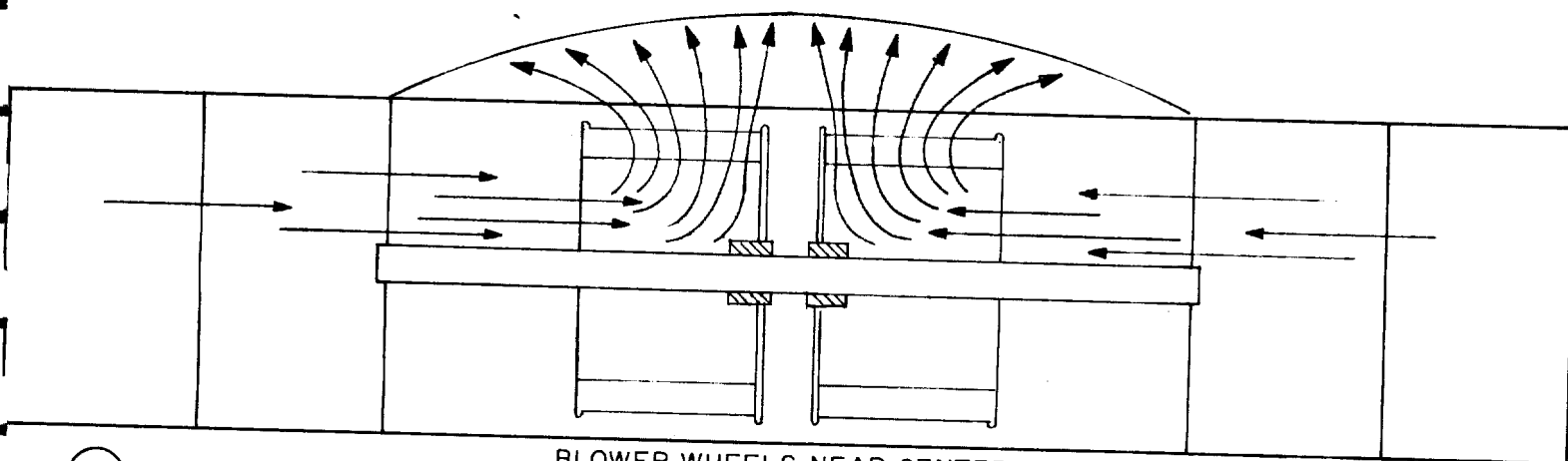
(A.)

BLOWER WHEELS FULL OUT



(B.)

BLOWER WHEELS SET INBOARD



(C.)

BLOWER WHEELS NEAR CENTER

Figure 4-2 Effect of Blower Wheel Position on Pressure Profile of Cushion

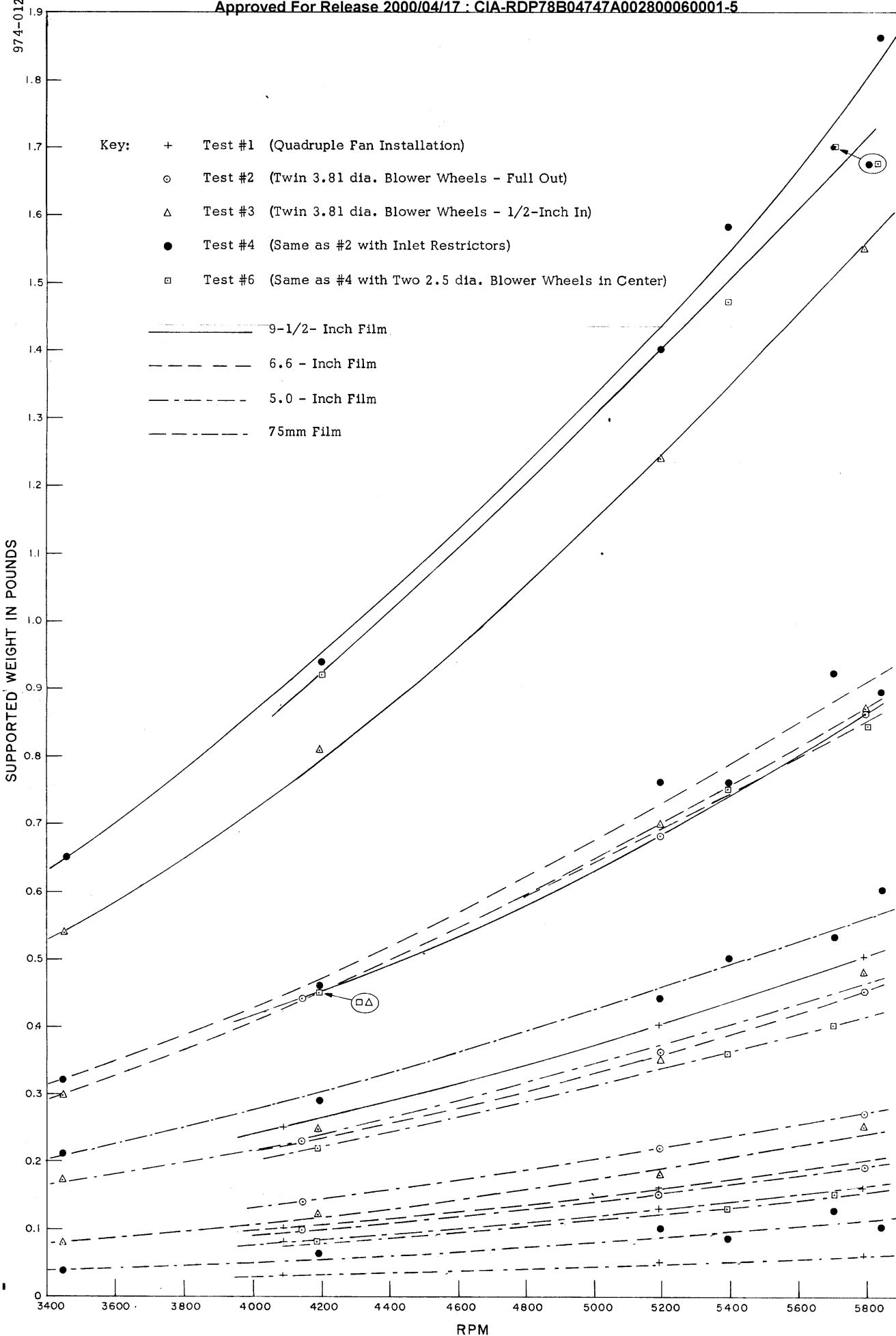


Figure 4-4. Supported Weight vs RPM for Different Configuration 4-17

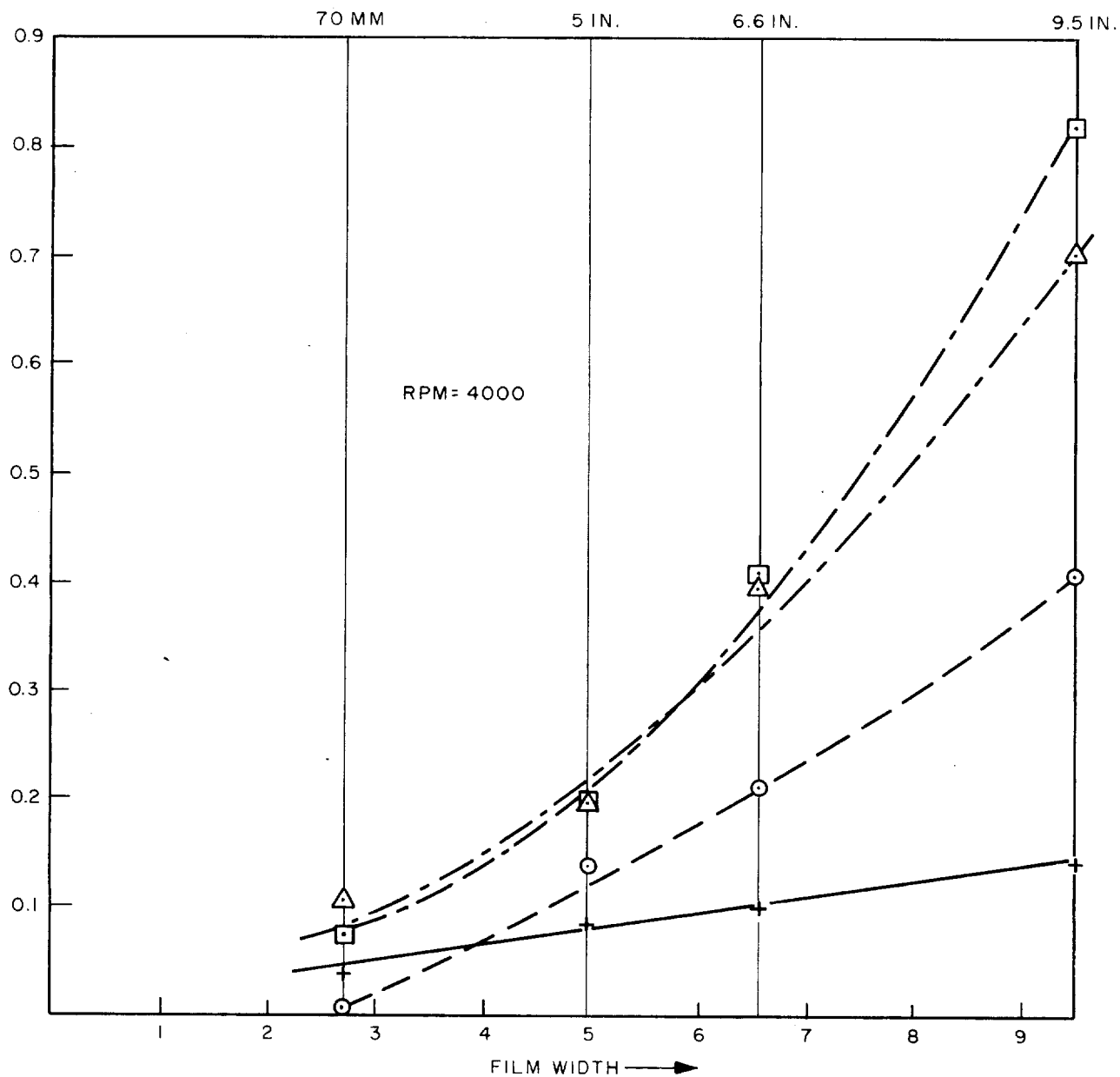


Figure 4-5. Configuration Lifting Capability at Constant RPM

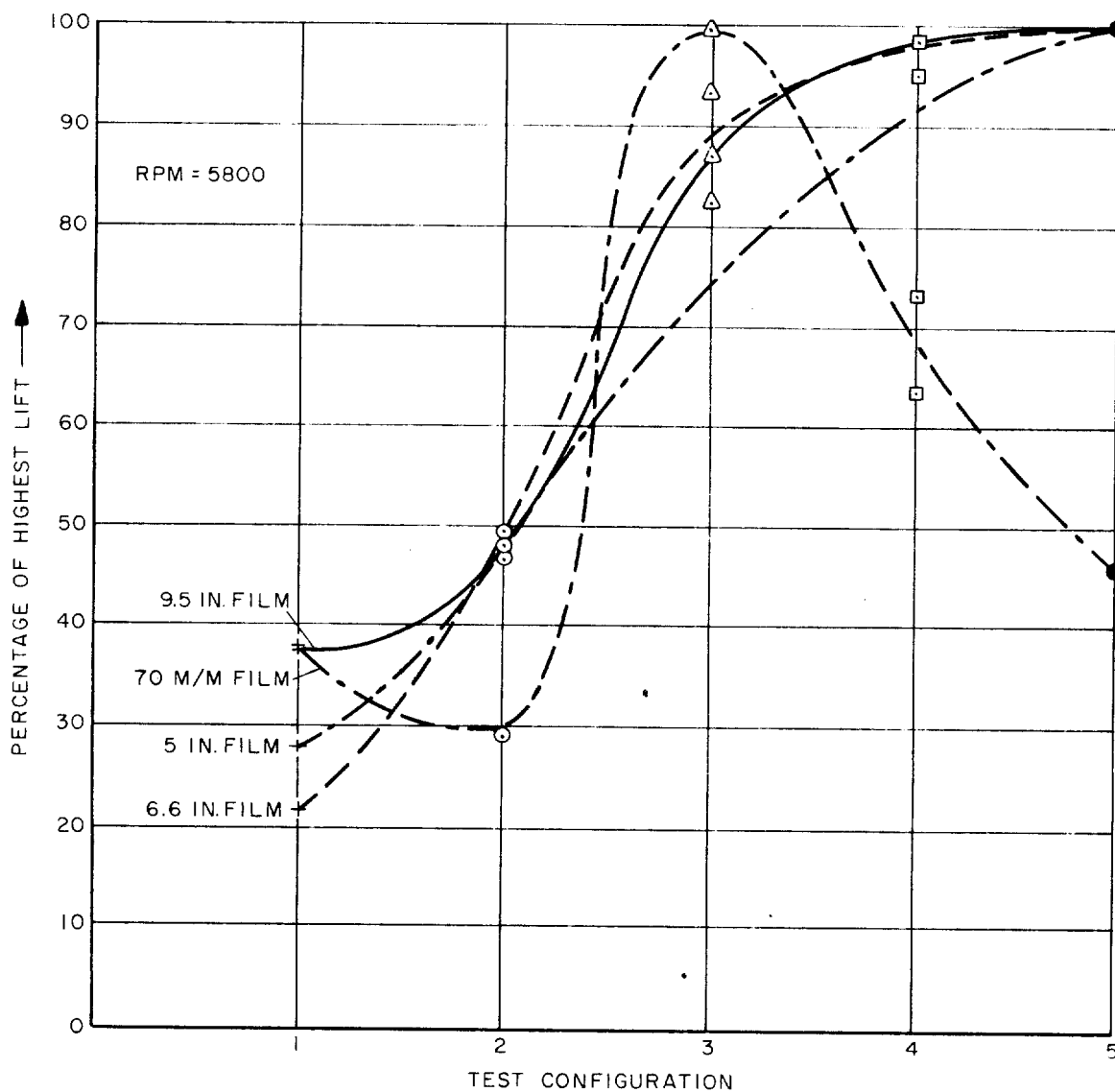


Figure 4-6 . Percentage of Lift for Various Test Configurations

TABLE 4-6 Percentage of Lift for Various Test Configurations

Test No.	9-1/2-inch		6.6-inch		5.0-inch		70m/m	
	Load Supported	Percentage Lift	Load Supported	Percentage Lift	Load Supported	Percentage Lift	Load Supported	Percentage Lift
1	0.5	38.1	.20	21.8	.16	27.9	.09	37.5
2	.86	48.3	.45	49.0	.27	47.0	.07	29.2
3	1.55	87.1	.87	94.6	.48	83.5	.24*	100
4	1.75	98.5	.88	95.7	.41	71.3	.15	62.5
5	1.78*	100	.92*	100	.575*	100	.11	45.8

* Maximum load supported for each film width is taken as 100 percent.

film is obtained in this configuration, with a good grouping of lifting characteristics for the other film widths. Against this, however, must be considered the instability of the 9-1/2-inch width film with regard to its centering capability.

4.4 TEST #4. TWIN 3.81-INCH DIAMETER BLOWER WHEELS - POSITION 1 WITH INTAKE RESTRICTORS

For this test, the blower wheels were restored to the same positions as Test #1, but, in an effort to eliminate or minimize the escape of air between the cage's internal diameter and the wheels, intake restrictors were added. These look the form of 4-1/2-inch outside diameter washers with an internal diameter the same as the blower wheel (Figure 4-1E). The wheels were operated through a range of speeds. The results are recorded in Table 4-7.

4.4.1. Efficiency of Configuration.

A comparison of lift efficiency between this configuration and previous test configurations can be made by reference to Figure 4-6, which shows a family of curves representing percentage of maximum lift for the various test configurations, at an impeller speed of 5800 rpm..It will be noted that while the percentage of maximum lift for 9-1/2, 6.6- and 5.0-inch film widths show an increase, the 70mm film shows a decrease in lift, as was noted during the actual testing. The test was made with the lower section of the bearing cage between the 8 o'clock and 4 o'clock stations filled in, and with the addition of a fixed aerodynamic fence on the top

TABLE 4-7

Load vs RPM and Unit Pressure Relationships for Test #4

Film Width	Impeller Speed (rpm)	Load Supported (lbs.)	Unit Area Pressure		Support Area (Sq. Ins.)
			P. S. I.	Ins. WG	
9-1/2-inch	3450	0.65	0.0144	0.399	45
	4200	0.94	0.0209	0.579	
	5200	1.40	0.0311	0.862	
	5400	1.58	0.0351	0.972	
	5710	1.70	0.0378	1.047	
	5850	1.86	0.0414	1.146	
6.6-inch	3450	0.32	0.0103	0.285	31
	4200	0.46	0.0148	0.410	
	5200	0.76	0.0245	0.678	
	5400	0.76	0.0245	0.678	
	5710	0.92	0.0297	0.823	
	5850	0.89	0.0287	0.794	
5.0-inch	3450	0.21	0.0078	0.216	27
	4200	0.29	0.0107	0.296	
	5200	0.44	0.0163	0.452	
	5400	0.50	0.0185	0.512	
	5710	0.53	0.0196	0.543	
	5850	0.60	0.0222	0.615	
70m/m	3450	0.035	0.0027	0.075	13
	4200	0.065	0.005	0.138	
	5200	0.10	0.0077	0.218	
	5400	0.085	0.0065	0.180	
	5710	0.125	0.0096	0.266	
	5850	0.10	0.0077	0.213	

150-degree segment of each end of the cage. This fence, or barrier, acted as a restrictor to the flow of air from under the ends of 9-1/2-inch wide film, thereby effecting an increase in lift.

Satisfactory concentric film loops about the bearing were obtained with acceptable cushion stability.

4.5 TEST #5. TWIN 3.81-INCH DIAMETER BLOWER WHEELS WITH INTAKE FAIRINGS

In a further attempt to improve the efficiency of the blower wheel installations, inlet fairings were fitted to each end of the bearing cage to minimize drag and to reduce pressure loss due to air leakage past the wheel (Figures 4-1F and 4-8). The fairings were also designed to divert this air leakage through the screen to increase the pressure velocity at the ends of the bearing cage. The test bed was operated at 5800 rpm and all film widths were loaded to obtain a 1/8-inch cushion height.

TABLE 4-8 Load vs RPM and Unit Pressure Relationships for Test #5

Film Width	Impeller Speed (rpm)	Load Supported (lb)	Unit Area Pressure		Supported Area Sq. Ins.
			P. S. I.	Ins. WG	
9-1/2-inch	5800	1.72	0.0382	1.058	45
6.6-inch		1.23	0.0397	1.100	31
5.0-inch		0.85	0.0315	0.873	27
70m/m		-	-	-	13

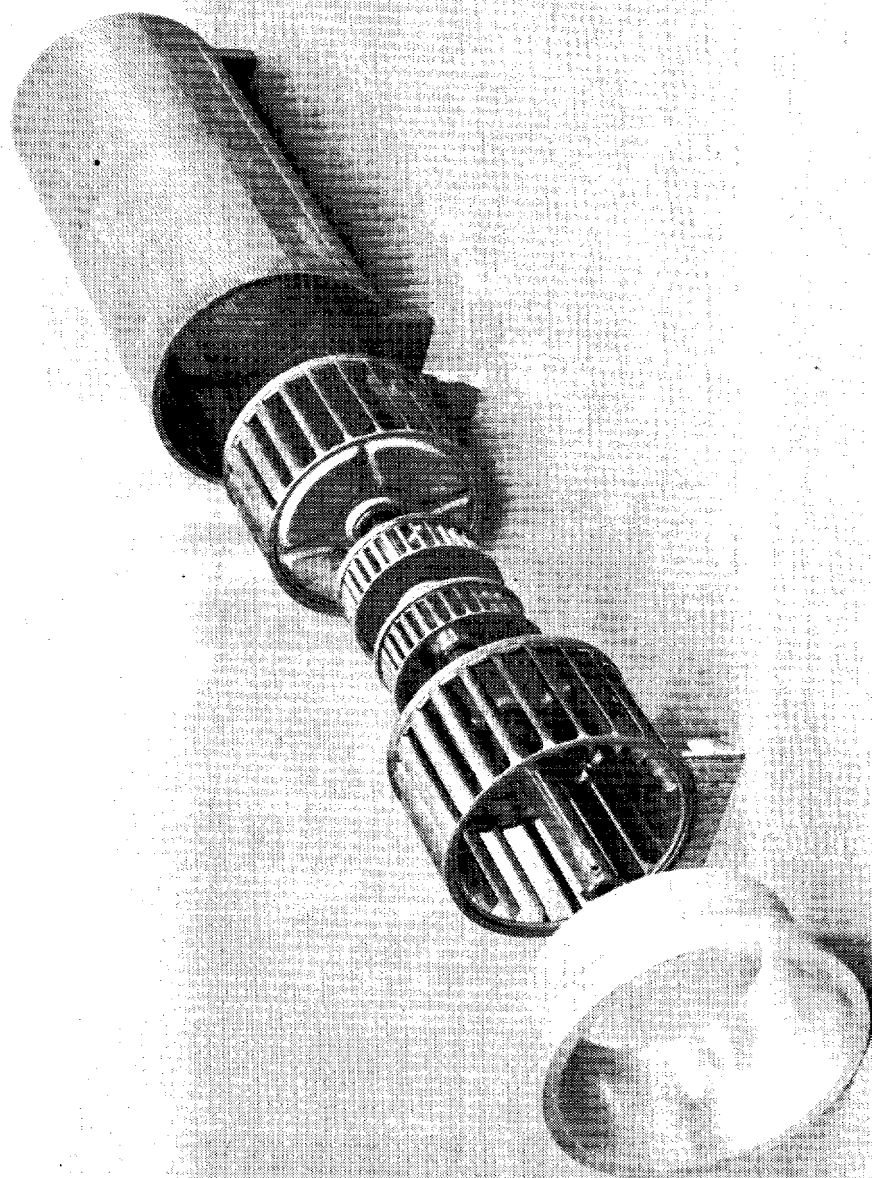


Figure 4-7. Inlet Fairing and Blower Wheel Have Been Moved Out of Cage to Show Relative Mounting Positions

With the lower portion of the cage, 8 o'clock to 4 o'clock stations covered over, and with the aerodynamic fences on the ends of the cage, the 9-1/2-inch film formed a concentric loop around the upper portion of the bearing cage. Without the fences, the film moved from side to side.

The 6.6- and 5.0-inch widths of film formed stable, concentric loops, although the 6.6-inch film exhibited a tendency to move from side to side.

The 70 m/m film would not lift clear of the cage even in an unloaded condition. Although the load lifting characteristics with the wider films exceeded that of previous tests, in all other aspects (such as stability of the 9-1/2- and 6.6-inch films), the failure to support 70 m/m in this configuration must be regarded as unsatisfactory.

To determine the pressure distribution, the cage was removed and replaced with a plastic tube. Manometer readings were taken at various points and showed that no pressure could be read in the center of the bearing. Since this configuration offered no advantage over those tested previously, no further testing was conducted.

4.6 TEST #6. TWIN 3.81-INCH DIAMETER BLOWER WHEELS WITH INTAKE RESTRICTORS AND TWO 2.50-INCH DIAMETER BLOWER WHEELS IN CENTER OF BEARING

For this test, the blower wheels were installed at the ends of the bearing cage with the intake restrictors fitted. In the previous tests, it was apparent that although good tracking depended upon a valley-shaped pressure profile instead of a crowned profile, it was also apparent that

the velocity pressure from the wheels was being discharged through the holes in the bearing cage in the area of the wheels, thus distributing little or no air flow through the center area of the cage with which to support the narrower film. To overcome this condition, two smaller blower wheels 2.50-inches in diameter were placed back-to-back in the center between the two larger wheels, so as to draw air into, or to impart velocity to, the air in this area (Figure 4-1D).

Tests were made on this configuration with the lower portion of the bearing cage covered as for previous tests. The results of the running tests made are given in Table 4-9. In all tests, the film was loaded to maintain a cushion of 1/8-inch height.

The two smaller wheels were (theoretically) capable of putting out 50 CFM (25 each) at 1.037-inches WG. A test run following this set-up proved satisfactory. All film widths tracked exceedingly well, carrying weights as shown in Table 4-9. The aerodynamic fence provided enough boundary to cause the 9-1/2-inch film to stay on center.

Pressure tests on the surface of the cage clearly show the pressure distribution, the "valley" being very obvious. See Figure 4-8.

TABLE 4-9

Load vs RPM and Unit Pressure Relationships for Test #6

Film Width	Impeller Speed (rpm)	Load Supported	Unit Area Pressure		Support Area (Sq. Ins.)
			P. S. I.	Ins. WG	
9-1/2-Inch	4200	0.92	0.0204	0.565	45
	5400	1.52	0.0338	0.937	
	5710	1.70	0.0378	1.047	
6.6-Inch	4200	0.45	0.0145	0.402	31
	5400	0.75	0.0246	0.682	
	5710	0.84	0.0271	0.750	
5.0-Inch	4200	0.22	0.0082	0.227	27
	5400	0.36	0.0133	0.368	
	5710	0.40	0.0148	0.410	
70 m/m	4200	0.08	0.0062	0.172	13
	5400	0.13	0.0100	0.277	
	5710	0.15	0.0115	0.319	

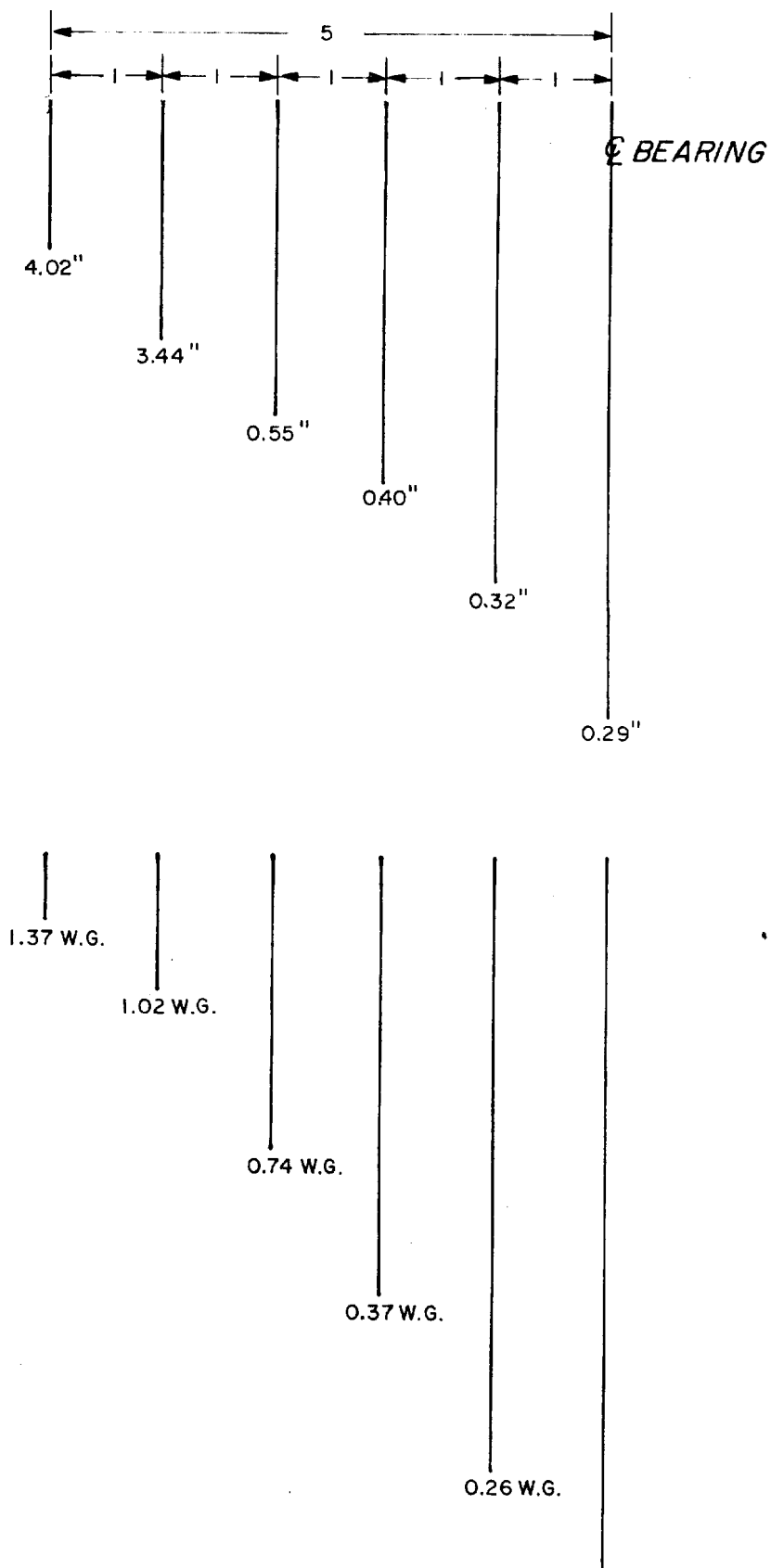


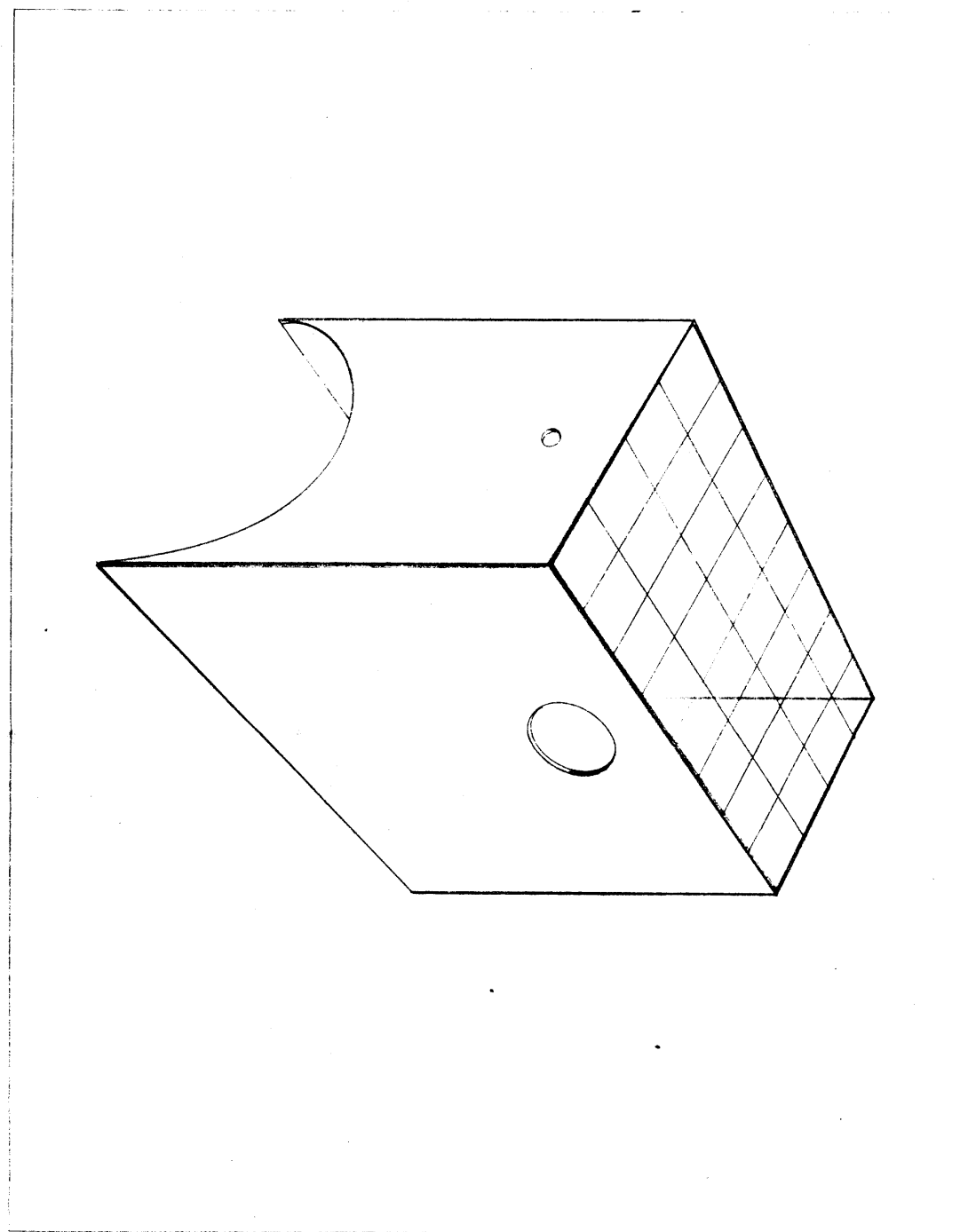
Figure 4-8. Pressure Tests at Surface of Bearing
 Approved For Release 2000/04/17 : CIA-RDP78B04747A002800060001-5

4.7 TEST #7. PRESSURE AND FLOW TESTS.

In order to measure the efficacy of the air bearing, a special stack was built of construction board (Figure 4-9). This stack was designed to fit snugly over the top hemicircular portion of the entire bearing, its outside dimensions at the mouth being 4-3/4 by 10-1/4-inches. The open top was then divided into 32 equal rectangles by means of a nylon grid. This enabled an accurate point-to-point traverse of the opening to be made with a flowmeter probe.

Two standard portable flowmeters were used for test purposes so that a volumetric comparison of results could be made. The first of these instruments was an Alnor "Velometer" Type 3002, Serial No. 24160, manufactured by the Alnor Instrument Company, Chicago, Illinois. It was equipped with various probes which enabled it to read velocities up to 10,000 fpm and static pressures up to 10-inches of water. The principle of operation is the deflection of a sapphire-jewel mounted, counter-balanced impingement vane.

The second instrument was an Anemostat "Anemotherm" air meter, Model 60, manufactured by the Anemostat Corporation of America, New York. Its readings depend on the cooling effect of a resistive element placed in various shielded probes in the effluent air. Besides velocity and static pressure, the instrument is capable of measuring temperature. Its scales cover the range 0-255°F with an accuracy of $\pm 1/2^\circ\text{F}$, 0-8000 fpm with an accuracy of ± 4 fpm for the low velocity

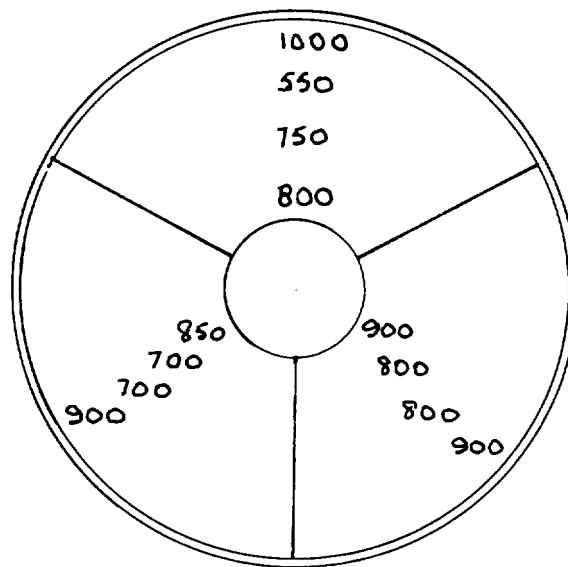


974-012-2

Figure 4-9. Discharge Stack with
Nylon Grid

scale and ± 5 fpm for the medium and high scales, and 0-10 inches WG. The latter readings are divided into two scales with an accuracy of $\pm .05$ inches WG on the 0-1.5 inch scale and $\pm .2$ on the 1-10 inch scale. In all cases, instrument static pressure readings were checked with an inclined manometer containing C.P. carbon tetrachloride.

With the stack attached to the blower cage by means of tape, readings were taken at the inlet throats (Figure 4-10) and the discharge plenum (Table 4-10).



Average Velocity = 837 fpm

Figure 4-10. Velocity Readings at Blower Inlet

TABLE 4-10
 Pressure Readings on Grid of Air Stack
 RPM = 5700
 (Each Reading Averaged from 3 Runs in 2 Places Each)

000	760	800	684	564	875	765	1025
711	527	400	473	553	390	550	912
1200	367	360	753	840	493	517	990
1330	706	606	794	995	738	704	1446

Average Velocity = 717 fpm

The cubic feet per minute flow was next calculated for the two inlet throats as follows:

$$D^2 \times \frac{\pi}{4} \times \frac{1}{144} = \text{Area in sq. ft.} \quad (4-6)$$

$$\frac{4.25^2 \times .7854}{144} = 0.0987 \text{ sq. ft.} \quad (4-7)$$

$$2 \times 837 \times 0.0987 = 165.0 \text{ cfm Intake} \quad (4-8)$$

The flow from the outlet plenum was then made:

$$\frac{10 \times 4.5 \times 717}{144} = 224.0 \text{ cfm Exhaust} \quad (4-9)$$

The discrepancy in the two readings must be assumed to be explainable by turbulence in the air streams and kinetic imbalance in a dynamic system involving a compressible medium, air. When the discharge plenum was completely blocked off and a static pressure read at the top of the stack, it agreed closely with the theoretical necessary to support the measured load at the same rpm. Adding a 1-1/2-inch plastic discharge pipe at the top of the stack, so that all effluent air was forced through it, did not reverse the inlet-discharge ratio.

SUMMARY AND CONCLUSIONS

5.1. Summary.

The scope of the research program into the feasibility of a self-powered air bearing did not permit an analytical study into the design and manufacture of air generators tailored specifically for this purpose. Standard, available, off-the-shelf equipment was therefore selected, and, as a result, a comparison of performance of the equipment in the test bed to that given in the manufacturer's performance data proved difficult since these latter data were based on results obtained under ideal conditions, with shrouds, intakes and housings designed specifically for the item of equipment. Air pressure distribution and flow checks versus the loads supported by various widths of film were therefore necessary to evaluate impeller characteristics as installed in the air bearing test bed. The problems of air pressure distribution and flow, while very similar to those encountered during evaluation of the "Rotatron" liquid bearing*, were magnified by the medium of air, this having a density of only 1/832 part of that of water, and, therefore, highly compressible. With the "Rotatron" bearing employing a medium with a density near that of water, which may be considered as incompressible, the problems of cushion stability were minimized.

In this regard liquid and gaseous fluids are quite different, since liquids offer a greater resistance to change of form or volume than gases which

25X1A

*Reference [REDACTED]

change rapidly in volume to fill the space in which they are retained.

It must be noted here that since a fluid or gas is not normally capable of maintaining itself in a fixed shape without the presence of restraining walls, then the loop of film formed over the bearing becomes an essential part of the bearing design itself, since without it, no volume of air would remain about the bearing. However, since the film loop is on an "imperfect" retainer inasmuch as it is open at the ends, and along the air outlet areas across its width, then the flow through these, with the pressure required to support the film loop at the required height above the bearing surface constitutes the spill, or loss, rate.

The basic function of the air generator used, then, is to maintain a unit area pressure against the film loop equal to the opposing load, while maintaining a velocity rate sufficient to replace the spill rate.

An air bearing, without a cage or envelope to provide a guard over the rotating impeller, is completely impractical; however, it was determined, during the testing of the "Rotatron" liquid bearing, that a cylindrical cage constructed of a perforated material performed not only this duty, but, more important functionally, that of a plenum. This design of cage was used in the air bearing tests and performed the same purpose of providing a plenum chamber. The air escaped from this plenum through the perforations and over the surface, providing a fluid surface retained by the film loop itself, with the total flow rate equal to the spill rate out of each open end and the sides. During the hydromatic

liquid bearing assessment, * strong emphasis was placed on the elimination of two essential features of a pressure plenum type air or liquid bearing. The first was the use of edge flanges to keep the film centered or in "track" on the bearing, and the second, a format changer that not only positioned the flanges to suit the required film width, but also closed off the slots or orifi outside the selected format to conserve energy. To eliminate the flanges, it was postulated that if the pressure profile were "crowned" in the same manner as a belt pulley, the film would remain centered on the bearing. This theory failed to work in practice, any movement of the film off-center in either direction was immediately magnified and caused an acceleration toward that end of the slot. An analysis of the forces showed that a "valley" pressure profile was required. This was proved successful in practice. In the tests conducted in this program (except the first with the four 4-inch diameter fans), the problem was reversed due to the positioning of the blower wheels. Insufficient pressure was generated in the center between the wheels to lift the narrower widths of film.

The diameter of the bearing was initially determined on the basis of the forces required to bend the film into a 180-degree loop about the bearing** and the diameter of available air handling equipment. The advantage of using the largest possible diameter of bearing is obvious if thought is

* Reference -

** Reference -

25X1A

given to the increased bearing surface area and the higher outputs at lower rpm obtained from the larger diameter blower wheels that can be employed. Six major configurations were tested and the performances analyzed on the basis of lift potential, self-centering capability, concentricity and stability of the film loop about the bearing.

The configurations were as follows:

- Test #1 Four 4-inch diameter fans.
- Test #2 Two 3.81-inch diameter blower wheels in the ends of the cage.
- Test #3 The same arrangement, but with the wheels positioned 1/2-inch inboard of Test #2.
- Test #4 The same arrangement and position as Test #2, but with intake flow restrictors.
- Test #5 The same arrangement as Test #2, but with intake fairings in the end of the cage.
- Test #6 Two 3.81-inch diameter blower wheels at the ends of the cage with intake flow restrictions and two 2.50-inch diameter blower wheels positioned in the center.

5.2. Conclusions.

The results of the tests conducted in this program demonstrate that the concept of a self-powered air bearing is feasible and worthy of continuing development. The program by no means covered all tests necessary to fully establish the aerodynamic parameters on which to

base the design of an idealized air bearing of this concept. Other configurations worthy of evaluation such as a full-length blower wheel with contoured blades, or a turbine arrangement of multi-blades of varying pitches and diameters were not investigated.

The perforated screen type cage, properly shrouded on the undersurface together with an impeller designed for the purpose, would unquestionably give better performance than was possible with the commercial units available for the tests reported herein. The impeller design should be such that it would be long enough to embrace the entire width of the bearing, tapering down from a maximum diameter at each end to a diameter at the center which would be of sufficient diameter to provide the necessary "valley" to center, or track all widths of film. The impeller could also be made structurally strong enough to permit higher rpm, thus improving the bearing load capabilities. It is conceivable that an impeller could be constructed which could operate at speeds as great as 10,000 rpm. In view of the relatively small horsepower requirements, a direct-coupled variable-speed motor could be used integrally with the bearing. A 10,000 rpm impeller speed would be capable, theoretically, of supporting almost three times the weight supported by this test bearing running at 5800 rpm.

25X1A

